Antagonism of Sphingosine 1-Phosphate Receptor-2 Enhances Migration of Neural Progenitor Cells Toward an Area of Brain Infarction

Atsushi Kimura, MD; Tsukasa Ohmori, MD; Yuji Kashiwakura, MSc; Ryunosuke Ohkawa, MSc; Seiji Madoiwa, MD; Jun Mimuro, MD; Kuniko Shimazaki, PhD; Yuichi Hoshino, MD; Yutaka Yatomi, MD; Yoichi Sakata, MD

Background and Purpose—We have previously shown that the sphingosine 1-phosphate (S1P)/S1P receptor-1 ($S1P_1R$) axis contributes to the migration of transplanted neural progenitor cells (NPCs) toward areas of spinal cord injury. In the current study, we examined a strategy to increase endogenous NPC migration toward the injured central nervous system to modify S1PR.

Methods—S1P concentration in the ischemic brain was measured in a mouse thrombosis model of the middle cerebral artery. NPC migration in vitro was assessed by a Boyden chamber assay. Endogenous NPC migration toward the insult was evaluated after ventricular administration of the $S1P_2R$ antagonist JTE-013.

Results—The concentration of S1P in the brain was increased after ischemia and was maximal 14 days after the insult. The increase in S1P in the infarcted brain was primarily caused by accumulation of microglia at the insult. Mouse NPCs mainly expressed $S1P_1R$ and $S1P_2R$ as S1PRs, and S1P significantly induced the migration of NPCs in vitro through activation of $S1P_1R$. However, an $S1P_1R$ agonist failed to have any synergistic effect on S1P-mediated NPC migration, whereas pharmacologic or genetic inhibition of $S1P_2R$ by JTE-013 or short hairpin RNA expression enhanced S1P-mediated NPC migration but did not affect proliferation and differentiation. Interestingly, administration of JTE-013 into a brain ventricle significantly enhanced endogenous NPC migration toward the area of ischemia.

Conclusions—Our findings suggest that S1P is a chemoattractant for NPCs released from an infarcted area and regulation of $S1P_2R$ function further enhances the migration of NPCs toward a brain infarction. (***Stroke*. 2008;39:3411-3417.)**

Key Words: migration ■ sphingosine 1-phosphate receptor-2 ■ sphingosine 1-phosphate ■ neural progenitor cells

Neural stem/progenitor cells (NPCs), self-renewing cells with the capacity to differentiate into neural cells, have been shown to exist mainly in 2 specific brain regions within the adult central nervous system (CNS): the subventricular zone (SVZ) and the hippocampal subgranular zone.[1] NPCs proliferate in the SVZ and migrate through it in a pattern reminiscent of the rostral migratory stream toward the olfactory bulb, where they differentiate into mature neurons.[2] NPCs also migrate to sites of brain injury. This may represent an adaptive response to limit or repair damage.[3,4] Newly generated NPCs are recruited from the SVZ to nearby areas of neural damage, and some show region-specific differentiation, known as neurogenesis.[3,4] A recent study showed that neurogenesis after brain injury is a meaningful response and that blockade of neurogenic cell division by irradiation worsens the outcome of cerebral ischemia.[5] Thus, a precise understanding of the mechanism underlying injury-mediated NPC migration may contribute to improving the effectiveness of stem cell–based therapies for CNS disorders.

Recently, we reported the importance of sphingosine 1-phosphate (S1P), a lysophospholipid mediator, for injury-mediated NPC migration.[6] S1P is currently attracting a great deal of attention as a bioactive sphingolipid that has various cellular functions and acts via the 7 transmembrane S1P receptors (S1PRs), $S1P_1R$ through $S1P_5R$.[7-9] We reported that the S1P concentration in the spinal cord increased after a contusion injury and contributed to the migration of transplanted NPCs in vivo via the $S1P_1R$.[6] In the current study, we show that S1P-mediated NPC migration toward an area of brain injury is enhanced by modulation of $S1P_2R$ function. We propose new therapeutic approaches to enhance the mobilization of endogenous NPCs toward areas of CNS injury.

Received January 14, 2008; final revision received April 21, 2008; accepted April 22, 2008.

From the Department of Orthopedic Surgery (A.K., Y.H.), the Center for Molecular Medicine (T.O., Y.K., S.M., J.M., Y.S.), and the Department of Physiology (K.S.), Jichi Medical University School of Medicine, Tochigi, and the Department of Clinical Laboratory Medicine (R.O., Y.Y.), Graduate School of Medicine, University of Tokyo, Tokyo, Japan.

Correspondence to Tsukasa Ohmori, MD, PhD, Research Division of Cell and Molecular Medicine, Center for Molecular Medicine, Jichi Medical University School of Medicine, 3111-1 Yakushiji, Shimotsuke, Tochigi 329-0498, Japan. E-mail tohmori@jichi.ac.jp

Stroke is available at http://stroke.ahajournals.org

DOI: 10.1161/STROKEAHA.108.514612

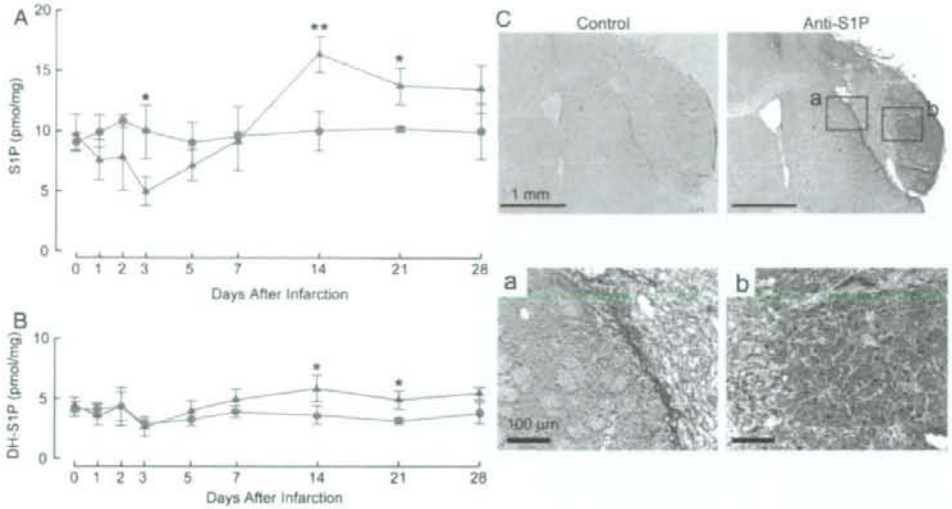

Figure 1. Alterations in S1P and dihydro-S1P concentrations after brain ischemia. The concentrations of S1P (A) and dihydro-S1P (B) in ischemic brain tissue (orange) or in contralateral control tissue (green) at various time points after brain ischemia were measured by high-performance liquid chromatography. Data represent mean±SD (n=3). $^{*}P<0.05$, $^{**}P<0.001$, 2-tailed Student's *t* test. C, Distribution of S1P in the brain 14 days after injury. Sections were immunostained with an antibody against S1P and visualized with Vector SG (black; anti-S1P). Counterstaining was carried out with Nuclear Fast Red (red). The same section stained with an isotype-matched control antibody is also shown (Control). Higher magnifications of the numbered boxed regions are shown in the lower panel.

Materials and Methods

Materials, measurement of S1P, immunohistochemistry, methods for migration, cell proliferation, NPC differentiation, construction of a lentiviral vector, and reverse transcription–polymerase chain reaction (RT-PCR) are described in detail in the supplemental materials, available online at http://stroke.ahajournals.org.

Photochemically Induced Brain Infarction

All animal procedures were approved by the institutional animal care and concern committee at Jichi Medical University. Animal care was performed in accordance with the committee's guidelines. C57BL/6 female mice (8 to 12 weeks old) were purchased from Japan SLC (Shizuoka, Japan). Thrombosis of the middle cerebral artery (MCA) in mice was performed as described.[10] In brief, mice were anesthetized with 1.7% to 2.0% isoflurane and the temporal muscle was transected to expose the skull. The left distal MCA could be observed through the skull. Photoillumination was achieved with a xenon lamp (model L4887–03; Hamamatsu Photonics, Hamamatsu, Japan) via an optic fiber with a focus. The light was focused onto the MCA over the intact skull at a power of 2.3×10^{6} lux. The photosensitizing dye Rose Bengal was simultaneously administered at a dose of 20 mg/kg IV within 5 minutes of laser irradiation.

Cell Culture

Mouse NPCs were isolated and cultured, as described previously.[6] In brief, the forebrains of E14.5 mouse embryos were isolated and mechanically dissociated into a suspension of single cells. The dissociated cells were cultured in Dulbecco's modified Eagle's medium/F12 supplemented with B27 supplement (Invitrogen, Carlsbad, Calif), 20 ng/mL basic fibroblast growth factor, and 20 ng/mL endothelial growth factor. The cells were used for experiments between passages 2 and 4.

Infusion of JTE-013 Into Brain Ventricles

For studies involving pharmacologic blockade of $S1P_2R$, 0.25 μL/h Alzet Minipumps (Durect Corp, Cupertino, Calif) were used for drug delivery. Empty pumps with flow moderators were weighed, filled with 1 mmol/L JTE-013 or phosphate-buffered saline (containing the same concentration of dimethyl sulfoxide as control), and then reweighed. Flow moderators were connected to a catheter (Alzet brain infusion kit 2; Durect Corp), which was connected to an infusion cannula. Pumps were stored overnight at 37°C in sterile saline to prime drug release. Two days after MCA thrombosis was induced, mice were anesthetized with isoflurane and placed in a small-animal stereotaxic frame. JTE-013 infusion during the acute phase of infarction may change the infarct size because inhibition of $S1P_2R$ is reported to affect vascular function.[11,12] Hence, we started the JTE-013 infusion 2 days after ischemia. The scalp was shaved, cleaned, and opened with a scalpel. A small burr hole was drilled 1 mm lateral and 0.2 mm caudal from the bregma. The catheter was lowered into the left ventricle (depth, 2.5 mm ventral) and affixed with dental cement, and the opening was sutured shut. Mice were euthanized by decapitation after 14 days. Cannula placement was verified by direct observation by cutting an insertion point. Once confirming the correct insertion, we proceeded to histologic analysis. The transverse sections (0.5 mm forward of the bregma) were analyzed to assess NPC migration in vivo. Endogenous NPC migration was detected by immunostaining of NPCs with an anti-doublecortin (DCX) polyclonal antibody (Santa Cruz Biotechnology). The distance to the ischemic area from the SVZ was separated into 3 parts (0 to 300 μm, 301 to 600 μm, and 601 to 900 μm). The DCX-positive area in each part was quantified with the use of Scion Image for Windows (Scion Corp). For 3-dimensional counting of migrated cells, 3 separate sections (0.5 mm, 0.7 mm, and 0.9 mm forward of the bregma) were prepared for analyses. To count the number of DCX-positive cells, the number of nuclei stained with DAPI in the DCX-positive area was manually counted by a blinded observer and expressed as the total number of DCX-positive cells in each area.

Results

Changes of S1P Concentration After Brain Infarction

To investigate the physiologic role of S1P in ischemic stroke, brain S1P concentrations were measured in a mouse model of brain ischemia. After brain infarction by photochemical induction of thrombosis in the distal MCA, most glial cells and neurons in the affected brain would be dead during the acute

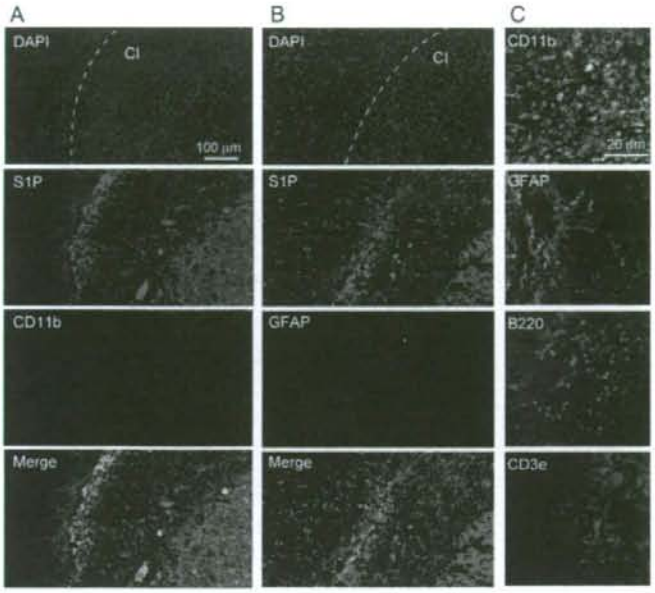

Figure 2. Localization of S1P after brain ischemia. Sections obtained from the brain 14 days after the insult were double-immunostained for CD11b and S1P (A) or glial fibrillary acid protein and S1P (B). Nuclear localization was simultaneously examined by DAPI staining. The merged images show colocalization of CD11b and S1P or of glial fibrillary acid protein and S1P. Areas of infarct are separated by a dotted line. CI indicates cerebral infarction). C, Representative images obtained from S1P (green) and merged with CD11b, glial fibrillary acid protein, B220, and CD3e (red) at higher magnification are shown.

phase of infarction. Reflecting this cell deterioration, S1P content was significantly decreased 3 days after infarction (Figure 1A). Interestingly, S1P content in the ischemic brain was significantly increased thereafter and reached a maximum 14 days after ischemia (Figure 1A). On the other hand, changes in dihydro-S1P concentration after ischemia were marginal (Figure 1B). Immunohistologic analysis with an anti-S1P antibody confirmed that the site of infarction contained a large amount of S1P (Figure 1C). S1P was highly expressed at the boundary zone and in the central core of the infarct (Figure 1C).

Next, we examined the cellular location of the elevated S1P content after brain infarction by immunohistochemistry. Destruction of the normal structure of the CNS and accumulation of microglia and immunoreactive cells of nonneural lineages expressing CD11b were observed after the insult (Figure 2A). S1P was highly expressed in the region of microglia accumulation in the infarct area and boundary zone (Figure 2A). On the other hand, astrocytes expressing glial fibrillary acid protein (GFAP) accumulated primarily at the boundary zone, whereas S1P immunoreactivity was partly colocalized, but S1P in the infarcted area was not (Figure 2B). As expected, few microtubule-associated protein 2 (MAP-2)–positive neurons were observed in the insult areas (data not shown). As well, most S1P immunoreactivity did not merge into B lymphocytes (B220) and T lymphocytes (CD3e; Figure 2C) in the infarcted area. These data suggest that microglia that accumulate at the site of injury are the main sources responsible for S1P elevation, whereas astrocytes might partly contribute to the increase in S1P in the boundary zone.

Expression of S1PR in Mouse NPCs

Many if not all of the biologic responses induced by S1P are mediated by its cell surface receptors, ie, S1PRs (S1P$_1$R through S1P$_5$R).[8,9] Next, we examined the expression of S1PRs in several adult mouse tissues and NPCs. Although S1P$_1$R seemed to be ubiquitously expressed, the patterns of S1PR expression were quite different among the tissues examined (Figure 3A). In this study, the NPCs expressed all known S1PRs (Figure 3A); real-time, quantitative RT-PCR analysis of NPCs revealed that S1P$_1$R and S1P$_2$R were the most highly expressed (Figure 3B).

Migration of NPCs Toward S1P

We next evaluated the effects of S1P on NPC migration. As shown in Figure 4A, S1P-induced migration resulted in a

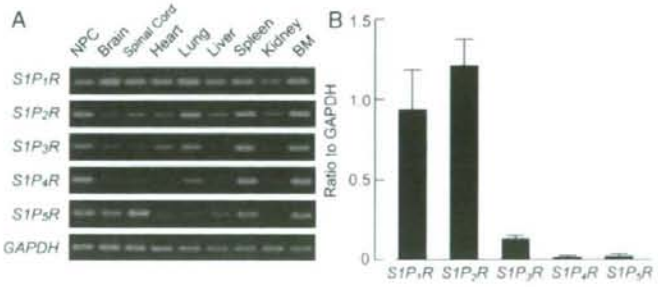

Figure 3. Expression of S1PRs in murine NPCs. A, RT-PCR analyses of transcripts derived from the genes for *S1P$_1$R* to *S1P$_5$R* in NPCs and in various mouse tissues. As a control, RT-PCR analysis for the mouse glyceraldehyde 3-phosphate dehydrogenase transcript was performed simultaneously. BM indicates bone marrow. B, mRNAs for the *S1P1R* to *S1P5R* genes in NPCs were quantified by real-time quantitative RT-PCR. Data represent mean±SD (n=3 per group).

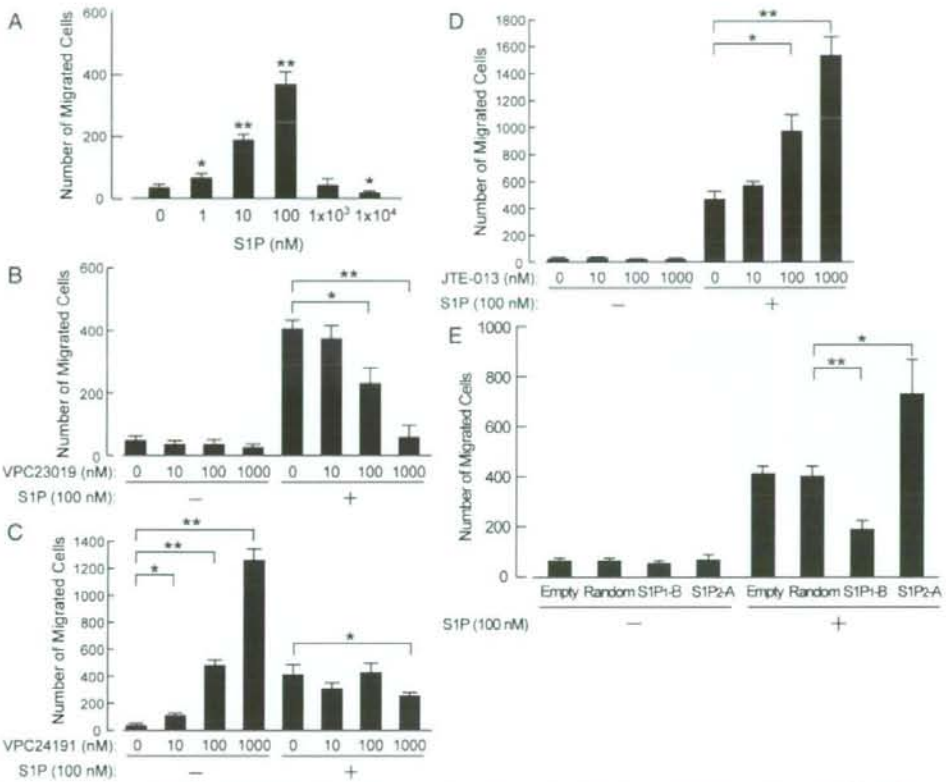

Figure 4. Modulation of NPC migration by agonists and antagonists for S1PR and by shRNA expression in vitro. A, NPC migration was assessed with use of a modified Boyden chamber assay. The indicated concentrations of S1P were placed in each lower chamber, and NPCs were allowed to migrate for 12 hours (n=3). B–D, NPC migration toward VPC23019 (B), VPC24191 (C), or JTE-013 (D), alone or in combination with 100 nmol/L S1P, was examined (n=3). E, NPCs were transduced with a lentiviral vector expressing no shRNA sequence (Empty), a random sequence (Random), an $S1P_1R$ sequence (S1P1B), or an $S1P_2R$ sequence (S1P2A). Transduced NPC migration with or without 100 nmol/L S1P was examined (n=3). Data represent mean±SD. *$P<0.05$, **$P<0.01$, 2-tailed Student's t test.

bell-shaped concentration-response curve, and the maximal response was observed at 100 nmol/L. To explore which S1PRs were involved in S1P-mediated NPC migration, we used 2 S1P-related synthetic compounds, VPC23019 and VPC24191. VPC23019 acts as a competitive inhibitor of $S1P_1R$ and $S1P_3R$ but partly stimulates $S1P_4R$ and $S1P_5R$.[13] On the other hand, VPC24191 is an agonist against $S1P_1R$ and $S1P_3R$. VPC23019 failed to induce NPC migration and abolished migration toward S1P (Figure 4B). VPC24191 by itself dramatically enhanced NPC migration in a concentration-dependent manner (Figure 4C). Interestingly, the addition of S1P inhibited the NPC migration elicited by a higher concentration of VPC24191 (1 to 10 μmol/L; Figure 4C). These data suggest that $S1P_1R$ is the primary receptor involved in S1P-mediated NPC migration, in support of our previous study,[6] but also indicated that other S1PRs can regulate the $S1P_1R$-mediated response.

We next focused on $S1P_2R$, a receptor that is responsible for inhibition of migratory responses.[14,15] Although JTE-013, a specific antagonist of $S1P_2R$, had no effect on NPC migration, S1P-mediated migration modulated by JTE-013 reached that induced by VPC24191 (Figure 4D). Similar results were observed after expression of short hairpin (sh) RNA: short interfering RNA against $S1P_1R$ ($S1P_1B$) inhibited S1P-mediated NPC migration, whereas $S1P_2R$ knockdown ($S1P_2A$) significantly enhanced the migration of NPCs elicited by S1P (Figure 4E). Considering that the concentration of S1P increased in the ischemic area, modulation of $S1P_2R$ instead of $S1P_1R$, could be a more practical approach to increase the mobilization of NPCs.

To examine whether inhibition of $S1P_2R$ affects other stem cell properties, we examined the effects of JTE-013 on the proliferation and differentiation of NPCs. S1P reportedly induced cell differentiation and proliferation[16]; however, S1P had only a marginal effect on NPC proliferation and differentiation in this study (Figure 5), and JTE-013 was without effect (Figure 5). These data suggest that modulation of $S1P_2R$ enhances S1P-mediated migration of NPCs without the loss of cell viability and the potential to differentiate.

Involvement of $S1P_2R$ in Endogenous NPC Migration

Finally, we attempted to increase the mobilization of endogenous NPCs by $S1P_2R$ antagonism. After infarction, we analyzed

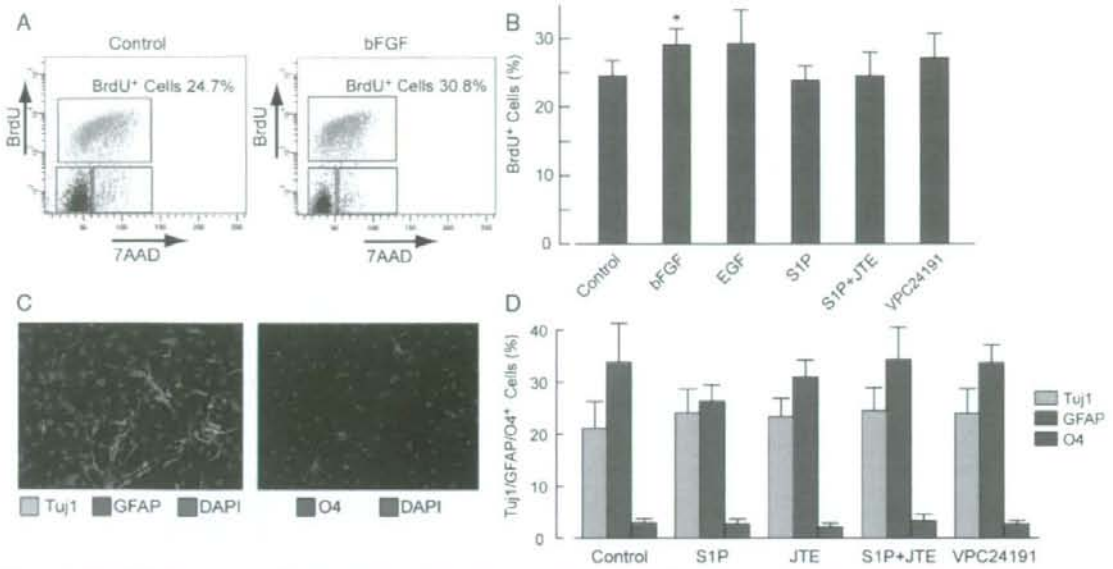

Figure 5. The S1P$_2$R antagonist JTE-013 had no affect on the proliferation and differentiation of NPCs. A, Bromodeoxyuridine incorporation was analyzed by flow cytometry after stimulation without (Control) or with 20 ng/mL basic fibroblast growth factor for 1 hour. Representative flow cytometry data are shown. B, Bromodeoxyuridine incorporation stimulated without (Control) or with 20 ng/mL basic fibroblast growth factor, 20 ng/mL endothelial growth factor, 1 μmol/L S1P, 1 μmol/L S1P and 1 μmol/L JTE-013, or 1 μmol/L VPC23419 was quantified. Data represent mean±SD (n=4). C, NPCs were cultured in the presence of 1% serum for 5 days, and lineage-specific differentiation was observed by immunocytochemistry. Representative data of double staining against Tuj1 and glial fibrillary acid protein (left) and single staining with O4 (right) is shown. D, The ratio of lineage-specific differentiation with addition of the indicated agent was quantified. Data represent mean±SD (n=4). *P<0.05, 2-tailed Student's t test.

NPC migration from the lateral ventricle wall by immunofluorescence against DCX, a microtubule-associated protein that is specifically expressed in NPCs and immature neurons. We started continuous administration of JTE-013 into the ventricle 2 days after focal brain ischemia to examine whether targeting S1P$_2$R would enhance endogenous NPC migration toward the area of the insult (Figure 6A). NPCs expressing DCX migrated from the lateral ventricle wall and accumulated around the

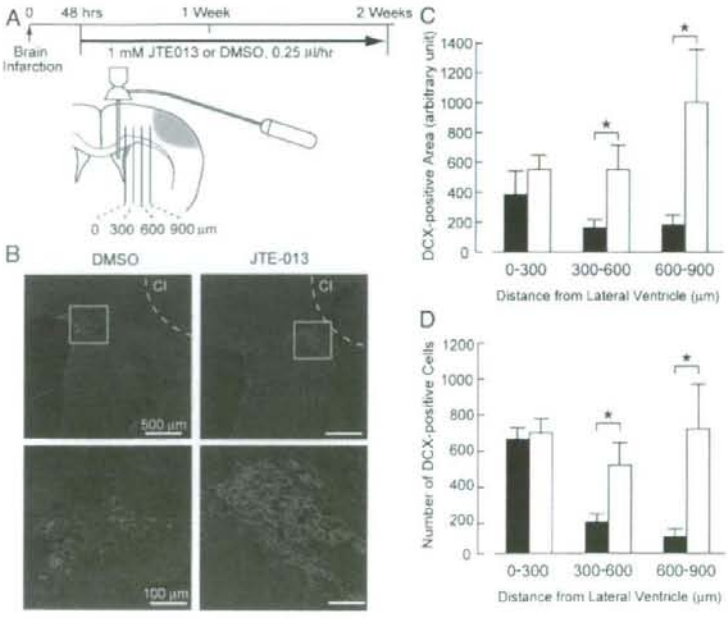

Figure 6. Enhancement of endogenous NPC migration toward areas of brain ischemia by ventricular administration of the S1P$_2$R antagonist JTE-013. A, Schematic presentation of the procedure and quantification of migrated DCX-positive cells. Two days after brain infarction, vehicle (dimethyl sulfoxide) or JTE-013 was continuously infused into the cerebral lateral ventricle. Histologic analysis of DCX was done at day 14. The distance to the ischemic area from the SVZ was separated into 3 parts (0 to 300 μm, 301 to 600 μm, and 601 to 900 μm). B, Representative data of histologic analyses of DCX are shown (red). Higher magnifications of the boxed regions are shown in the lower panel. Areas of infarction are separated by a dotted line (CI). C, Each area of DCX-positive cells was separately quantified in the section at 0.5 mm forward of the bregma. Vehicle is indicated by black bars; JTE-013, by white bars. Data represent mean±SE (n=6 per each group). D, Migrated DCX-positive cells were stereologically assessed by counting the total number of cells in 3 separate cross sections (0.5 mm, 0.7 mm, and 0.9 mm forward of the bregma). Vehicle is indicated by black bars; JTE-013, by white bars. Data represent mean±SE (n=3 per each group). *P<0.05, 2-tailed Student's t test.

ischemic area (Figure 6B). Interestingly, NPC migration toward the ischemic area was dramatically enhanced by ventricular infusion of JTE-013 (Figures 6B through 6D). Administration of JTE-013 into ventricles could diffuse into many areas in the brain and so might affect many neurologic functions; many kind of neural cells reportedly express S1PRs, including $S1P_2R$.[17] However, enhanced NPC migration after administration of JTE-013 was not observed in the contralateral side of the infarct (data not shown). These data suggest that pharmacologic inhibition of $S1P_2R$ in NPCs by JTE-013 promotes endogenous NPC migration toward the areas of brain ischemia where S1P has increased.

Discussion

Migration of NPCs is important not only for development of the embryonic nervous system but also for repair of the nervous system after injury.[3,4] Identifying candidate molecules that could play a role in NPC migration is crucial for understanding proper tissue formation by newly formed neural cells, as well as for developing novel therapies to promote neural repair after CNS injury.[18,19] We previously showed a role for S1P in NPC migration toward a pathologic area of the CNS and proposed that elevation of S1P at the site of injury was a guiding factor for NPC migration.[6] Here, we reveal that $S1P_2R$ is a potential target for strategies aiming to increase NPC migration after brain ischemia.

We have already shown that $S1P_1R$ contributes to NPC migration toward areas of high S1P expression in the injured CNS.[6] This occurs in a variety of cell types through Gi-mediated Rac activation,[20,21] whereas $S1P_2R$ abolishes migration after the coupling of $S1P_2R$ to the $G_{12/13}$/Rho pathway.[11,22] The $S1P_2R$ abolished migration not only through $S1P_1R$ but also other types of receptors for growth factor.[14,15] Overactivation of the Rho/Rho-kinase pathway is thought to be 1 of the important mechanisms that strongly inhibit cell migration.[11] These data present 2 strategies for the induction of NPC migration to a site of injury: elevation of $S1P_1R$ signaling or blockade of $S1P_2R$ signaling. However, the $S1P_1R$-specific agonist failed to enhance NPC migration in the presence of S1P, suggesting that activation of $S1P_1R$ itself could not overcome the inhibitory effect of $S1P_2R$ in NPCs. Considering that the concentration of S1P increases at the site of an insult, modulation of $S1P_2R$ function could be a more practical approach for the mobilization of NPCs when compared with modulation of $S1P_1R$ function. We confirmed the involvement of $S1P_2R$ in in vitro NPC migration by RNA interference experiments; however, the effects of JTE-013 unrelated to $S1P_2R$ antagonism could not be completely eliminated because JTE-013 is reported to inhibit vasoconstriction through unknown mechanism(s) independent of the $S1P_2R$.[23] Further studies with gene-deficient mice would be required to confirm the full effects of $S1P_2R$ inhibition.

Migration of NPCs is an important process in neurogenesis.[4] The neural stem cells of the SVZ are the principal source of NPCs, which form chainlike structures and migrate laterally toward the injured striatal regions before differentiating into mature neurons.[3,4,19] Our data suggest that local elevation of S1P concentration after brain ischemia acts as an activation signal for NPCs in the SVZ and that modulation of $S1P_2R$ function could enhance endogenous NPC migration. Recent studies have suggested that endogenous NPC migration and angiogenesis are mechanistically linked in the nervous system; neuroblast cells migrate toward blood vessels in areas undergoing early vascular remodeling.[24,25] Vascular endothelial growth factor, a major angiogenic factor that acts as a guiding factor for endothelial progenitors, is an attractive guidance cue for the migration of undifferentiated NPCs.[26,27] Our data show that S1P, another important angiogenic factor,[20] also guides the migration of NPCs, suggesting a mechanistic link between NPC migration and angiogenesis via the S1P/S1PR axis in the nervous system.

The change in S1P concentration after brain ischemia is quite different from that of known inflammatory cytokines, chemokines, and growth factors. Intercellular adhesion molecules, including intercellular adhesion molecule-1 and selectins, are rapidly induced 3 to 6 hours after ischemia and peak at 6 to 12 hours.[28,29] The expression of adhesion molecules on microvessels promotes neutrophil recruitment and trafficking into the brain.[28,29] Adhesion molecules and inflammatory mediators play a role in focal ischemic brain injury. In this study, the concentration of S1P was gradually enhanced at the site of ischemia, and S1P was highly expressed at the site of microglia accumulation. The gradual increase in S1P led us to postulate that it plays an important role in regeneration after CNS injury. Microglia reportedly release an unidentified chemoattractant(s) for NPCs after CNS injury and thus play an important role in directing the replacement of damaged or lost cells in the CNS.[30] Recently, selective ablation of microglial cells was shown to exacerbate ischemic injury in the brain, suggesting that microglial cells serve as an endogenous pool of neurotrophic molecules.[31] Because S1P enhances the migration of NPCs, we postulate that S1P is a physiologic, neuroprotective substance released from microglia.

An issue that remains to be addressed is what stimulates S1P biosynthesis after injury. A common product of sphingolipid breakdown is ceramide, which is generated primarily by hydrolysis of membrane sphingomyelin.[32] Ceramide can be further catabolized by ceramidases to generate sphingosine, which can be phosphorylated through the action of sphingosine kinase, generating S1P.[33] Sphingosine kinase activity in the brain was recently reported to increase 24 hours after ischemia in a mouse model of MCA occlusion[34]; however, those increases were not necessarily the same as the S1P concentration in our study. As well, if elevation of sphingosine kinase activity accounts for the increase in S1P concentration after insult, the concentration of dihydro-S1P would increase because dihydrosphingosine is phosphorylated by sphingosine kinase isozymes to an extent similar to that of naturally occurring sphingosine.[35,36] One possible mechanism is sphingomyelin breakdown after phagocytosis of neural cells by activated microglia. Microglial activation and phagocytic potential are reported to occur gradually between 1 and 12 weeks after an ischemic insult.[37] Activated microglial cells phagocytose dead neural cells and may induce sphingomyelin breakdown during the neuroregeneration phase. Investigations into the precise mechanisms of injury-mediated S1P elevation and sphingosine metabolism at injury sites are now under way in our laboratory.

Summary

In summary, increased S1P at the site of brain infarction acts as a chemoattractant for NPCs. Although activation of S1P$_1$R failed to enhance NPC migration in the presence of S1P, S1P$_2$R, a specific antagonist of the migration-inhibitory receptor, upregulates migration responses induced by S1P and augments endogenous NPC migration toward the ischemic insult. These data suggest that S1P$_2$R blockade is a promising candidate to enhance NPC migration toward sites of brain infarction. Further studies in gene-deficient mice will be needed, as will behavioral and functional analyses after the administration of S1P$_2$R antagonists for treatment of ischemic stroke.

Acknowledgments

We thank N. Matsumoto, M. Ito, and A. Ishiwata for their excellent technical assistance.

Sources of Funding

This work was supported by the Takeda Science Foundation; grants-in-aid for scientific research from the Ministry of Education and Science; Health and Labour science research grants for research from the Ministry of Health, Labour and Welfare; and grants for High-Tech Center Research projects for private universities, with a matching fund subsidy from the Ministry of Education, Culture, Sports, Science, and Technology, 2002–2006.

Disclosures

None.

References

1. Gage FH. Mammalian neural stem cells. *Science*. 2000;287:1433–1438.
2. Hagg T. Molecular regulation of adult CNS neurogenesis: an integrated view. *Trends Neurosci*. 2005;28:589–595.
3. Lindvall O, Kokaia Z, Martinez-Serrano A. Stem cell therapy for human neurodegenerative disorders—how to make it work. *Nat Med*. 2004; 10(suppl):S42–S50.
4. Okano H, Sakaguchi M, Ohki K, Suzuki N, Sawamoto K. Regeneration of the central nervous system using endogenous repair mechanisms. *J Neurochem*. 2007;102:1459–1465.
5. Raber J, Fan Y, Matsumori Y, Liu Z, Weinstein PR, Fike JR, Liu J. Irradiation attenuates neurogenesis and exacerbates ischemia-induced deficits. *Ann Neurol*. 2004;55:381–389.
6. Kimura A, Ohmori T, Ohkawa R, Madoiwa S, Mimuro J, Murakami T, Kobayashi E, Hoshino Y, Yatomi Y, Sakata Y. Essential roles of sphingosine 1-phosphate/S1P1 receptor axis in the migration of neural stem cells toward a site of spinal cord injury. *Stem Cells*. 2007;25:115–124.
7. Herr DR, Chun J. Effects of LPA and S1P on the nervous system and implications for their involvement in disease. *Curr Drug Targets*. 2007; 8:155–167.
8. Kluk MJ, Hla T. Signaling of sphingosine-1-phosphate via the S1P/EDG-family of G-protein-coupled receptors. *Biochim Biophys Acta*. 2002; 1582:72–80.
9. Spiegel S, Milstien S. Sphingosine-1-phosphate: an enigmatic signalling lipid. *Nat Rev Mol Cell Biol*. 2003;4:397–407.
10. Sugimori H, Yao H, Ooboshi H, Ibayashi S, Iida M. Krypton laser-induced photothrombotic distal middle cerebral artery occlusion without craniectomy in mice. *Brain Res Brain Res Protoc*. 2004;13: 189–196.
11. Lepley D, Paik JH, Hla T, Ferrer F. The G protein-coupled receptor S1P2 regulates Rho/Rho kinase pathway to inhibit tumor cell migration. *Cancer Res*. 2005;65:3788–3795.
12. Ohmori T, Yatomi Y, Osada M, Kazama F, Takafuta T, Ikeda H, Ozaki Y. Sphingosine 1-phosphate induces contraction of coronary artery smooth muscle cells via S1P2. *Cardiovasc Res*. 2003;58:170–177.
13. Davis MD, Clemens JJ, Macdonald TL, Lynch KR. Sphingosine 1-phosphate analogs as receptor antagonists. *J Biol Chem*. 2005;280: 9833–9841.
14. Okamoto H, Takuwa N, Yokomizo T, Sugimoto N, Sakurada S, Shigematsu H, Takuwa Y. Inhibitory regulation of rac activation, membrane ruffling, and cell migration by the G protein-coupled sphingosine-1-phosphate receptor EDG5 but not EDG1 or EDG3. *Mol Cell Biol*. 2000;20:9247–9261.
15. Osada M, Yatomi Y, Ohmori T, Ikeda H, Ozaki Y. Enhancement of sphingosine 1-phosphate-induced migration of vascular endothelial cells and smooth muscle cells by an EDG-5 antagonist. *Biochem Biophys Res Commun*. 2002;299:483–487.
16. Harada J, Foley M, Moskowitz MA, Waeber C. Sphingosine-1-phosphate induces proliferation and morphological changes of neural progenitor cells. *J Neurochem*. 2004;88:1026–1039.
17. Milstien S, Gude D, Spiegel S. Sphingosine 1-phosphate in neural signalling and function. *Acta Paediatr Suppl*. 2007;96:40–43.
18. Le Belle JE, Svendsen CN. Stem cells for neurodegenerative disorders: where can we go from here?. *BioDrugs*. 2002;16:389–401.
19. Picard-Riera N, Nait-Oumesmar B, Baron-Van Evercooren A. Endogenous adult neural stem cells: limits and potential to repair the injured central nervous system. *J Neurosci Res*. 2004;76:223–231.
20. Lee MJ, Thangada S, Claffey KP, Ancellin N, Liu CH, Kluk M, Volpi M, Sha'afi RI, Hla T. Vascular endothelial cell adherens junction assembly and morphogenesis induced by sphingosine-1-phosphate. *Cell*. 1999;99: 301–312.
21. Lee MJ, Thangada S, Paik JH, Sapkota GP, Ancellin N, Chae SS, Wu M, Morales-Ruiz M, Sessa WC, Alessi DR, Hla T. Akt-mediated phosphorylation of the G protein-coupled receptor EDG-1 is required for endothelial cell chemotaxis. *Mol Cell*. 2001;8:693–704.
22. Sugimoto N, Takuwa N, Okamoto H, Sakurada S, Takuwa Y. Inhibitory and stimulatory regulation of rac and cell motility by the G12/13-rho and Gi pathways integrated downstream of a single G protein-coupled sphingosine-1-phosphate receptor isoform. *Mol Cell Biol*. 2003;23: 1534–1545.
23. Salomone S, Potts EM, Tyndall S, Ip PC, Chun J, Brinkmann V, Waeber C. Analysis of sphingosine 1-phosphate receptors involved in constriction of isolated cerebral arteries with receptor null mice and pharmacological tools. *Br J Pharmacol*. 2008;153:140–147.
24. Louissaint A Jr, Rao S, Leventhal C, Goldman SA. Coordinated interaction of neurogenesis and angiogenesis in the adult songbird brain. *Neuron*. 2002;34:945–960.
25. Palmer TD, Willhoite AR, Gage FH. Vascular niche for adult hippocampal neurogenesis. *J Comp Neurol*. 2000;425:479–494.
26. Sun Y, Jin K, Xie L, Childs J, Mao XO, Logvinova A, Greenberg DA. VEGF-induced neuroprotection, neurogenesis, and angiogenesis after focal cerebral ischemia. *J Clin Invest*. 2003;111:1843–1851.
27. Zhang H, Vutskits L, Pepper MS, Kiss JZ. VEGF is a chemoattractant for FGF-2-stimulated neural progenitors. *J Cell Biol*. 2003;163:1375–1384.
28. Pantoni L, Sarti C, Inzitari D. Cytokines and cell adhesion molecules in cerebral ischemia: experimental bases and therapeutic perspectives. *Arterioscler Thromb Vasc Biol*. 1998;18:503–513.
29. Sharp FR, Lu A, Tang Y, Millhorn DE. Multiple molecular penumbras after focal cerebral ischemia. *J Cereb Blood Flow Metab*. 2000;20: 1011–1032.
30. Aarum J, Sandberg K, Haeberlein SL, Persson MA. Migration and differentiation of neural precursor cells can be directed by microglia. *Proc Natl Acad Sci U S A*. 2003;100:15983–15988.
31. Lalancette-Hebert M, Gowing G, Simard A, Weng YC, Kriz J. Selective ablation of proliferating microglial cells exacerbates ischemic injury in the brain. *J Neurosci*. 2007;27:2596–2605.
32. Pyne S, Pyne NJ. Sphingosine 1-phosphate signalling in mammalian cells. *Biochem J*. 2000;349:385–402.
33. Liu H, Chakravarty D, Maceyka M, Milstien S, Spiegel S. Sphingosine kinases: a novel family of lipid kinases. *Prog Nucleic Acid Res Mol Biol*. 2002;71:493–511.
34. Blondeau N, Lai Y, Tyndall S, Popolo M, Topalkara K, Pru JK, Zhang L, Kim H, Liao JK, Ding K, Waeber C. Distribution of sphingosine kinase activity and mRNA in rodent brain. *J Neurochem*. 2007;103:509–517.
35. Kohama T, Olivera A, Edsall L, Nagiec MM, Dickson R, Spiegel S. Molecular cloning and functional characterization of murine sphingosine kinase. *J Biol Chem*. 1998;273:23722–23728.
36. Liu H, Sugiura M, Nava VE, Edsall LC, Kono K, Poulton S, Milstien S, Kohama T, Spiegel S. Molecular cloning and functional characterization of a novel mammalian sphingosine kinase type 2 isoform. *J Biol Chem*. 2000;275:19513–19520.
37. Ito U, Nagasao J, Kawakami E, Oyanagi K. Fate of disseminated dead neurons in the cortical ischemic penumbra: ultrastructure indicating a novel scavenger mechanism of microglia and astrocytes. *Stroke*. 2007;38:2577–2583.

Phenotypic Correction of Hemophilia A by Ectopic Expression of Activated Factor VII in Platelets

Tsukasa Ohmori[1], Akira Ishiwata[1], Yuji Kashiwakura[1], Seiji Madoiwa[1], Katsuyuki Mitomo[2], Hidenori Suzuki[3], Mamoru Hasegawa[2], Jun Mimuro[1] and Yoichi Sakata[1]

[1]Research Division of Cell and Molecular Medicine, Center for Molecular Medicine, Jichi Medical University School of Medicine, Tochigi, Japan; [2]DNAVEC Corporation, Ibaraki, Japan; [3]Laboratory for Electron Microscopy, Tokyo Metropolitan Institute, Tokyo, Japan

Platelets are receiving much attention as novel target cells to secrete a coagulation factor for hemophilia gene therapy. In order to extend the application of platelet-directed gene therapy, we examined whether ectopic expression of activated factor VII (FVIIa) in platelets would result in an efficient bypass therapy to induce sufficient thrombin generation on platelet surfaces in mice with hemophilia A. Transduction of bone marrow cells with a simian immunodeficiency virus (SIV)-based lentiviral vector harboring the platelet-specific *GPIbα* promoter resulted in efficient transgene expression in platelets. FVIIa antigen was expressed in platelets by this SIV system; FVII transgene products were found to localize in the cytoplasm and translocate toward the sub-membrane zone and cell surface after activation. Although FVII antigen levels in platelets did not reach the therapeutic levels seen with FVIIa infusion therapy, whole-blood coagulation, as assessed by thromboelastography, was significantly improved in mice with hemophilia A. Further, we observed correction of the bleeding phenotype in mice with hemophilia A after transplantation, even in the presence of FVIII-neutralizing antibodies. Our results demonstrate that FVIIa-expressing platelets can strengthen hemostatic function and may be useful in treating hemophilia and other inherited bleeding disorders. These findings are comparable to the proven therapeutic effects of FVIIa infusion.

Received 8 February 2008; accepted 30 April 2008; published online 3 June 2008. doi:10.1038/mt.2008.117

INTRODUCTION

Platelets are differentiated anucleate cells whose functions are essential for hemostasis. Because platelets can circulate throughout the body, release a number of mediators on demand, and provide a scaffold for the coagulation cascade, the targeting of platelets as a circulating delivery system would seem a reasonable approach to genetic modification of hemostasis. The feasibility of such a platelet-directed approach was originally demonstrated by Poncz *et al.* in transgenic mice.[1] Platelet expression of urokinase-type plasminogen activator, using a platelet-specific *platelet factor-4* promoter, enabled urokinase-type plasminogen activator to be stored in platelets and then released within developing thrombi when the platelets became activated.[1] Further, platelet-specific expression of factor VIII (FVIII) can be achieved in a transgenic setting, with the resultant FVIII predominantly or exclusively stored in platelet granules rather than being released into the plasma.[2] In addition, Shi *et al.* have demonstrated that ectopically expressed FVIII in platelets can be used in the treatment of hemophilia with or without FVIII-neutralizing antibodies, and that targeted FVIII expression in platelets continues to support hemostasis even in the presence of high titers of FVIII-neutralizing antibodies.[3] We and others have applied this approach to gene therapy, and have demonstrated that transplantation of hematopoietic stem cells (HSCs) transduced with a lentiviral vector containing *human FVIII* driven by a platelet-specific promoter improves the hemostatic function of mice with FVIII-deficient hemophilia A, despite the levels of FVIII in their plasma being scant or undetectable.[4,5]

In order to further extend the application of platelet-directed gene therapy, we focused our attention on the extrinsic pathway initiated by tissue factor (TF). Assembly of TF and activated Factor VII (FVIIa) complexes on anionic phospholipids expressed on activated cell membranes is the most important initiation mechanism for blood coagulation.[6] Recently, recombinant human FVIIa (rhFVIIa: NovoSeven) has proven to be a highly successful alternative treatment for hemophilia patients.[7] Patients with a variety of other coagulation deficiencies that are characterized by impaired thrombin generation have been successfully treated with rhFVIIa.[8] In addition, liver-directed gene therapy with an adeno-associated virus vector equipped with hFVIIa achieved therapeutic plasma hFVIIa levels in a mouse model of hemophilia B, and phenotypic correction was observed when a murine FVIIa (mFVIIa) homolog was used.[9] In addition, it is possible that platelets that stably express FVIIa can efficiently induce hemostasis at the site of vascular injury in a variety of hemorrhagic disorders. In this study, we used gene therapy to examine whether platelet-specific FVIIa expression would result in an efficient bypass therapy for

Correspondence: *Tsukasa Ohmori or Yoichi Sakata, Research Division of Cell and Molecular Medicine, Center for Molecular Medicine, Jichi Medical University School of Medicine, 3111-1 Yakushiji, Shimotsuke, Tochigi 329-0498, Japan. E-mail: tohmori@jichi.ac.jp or yoisaka@jichi.ac.jp*

factor X activation, thereby generating sufficient thrombin on platelet surfaces in FVIII-deficient mice.

RESULTS

Enhanced green fluorescent protein expression in platelets after transplantation of HSCs transduced with a simian immunodeficiency virus lentiviral vector harboring the platelet *GPIbα* promoter

We have previously shown that transplantation of c-kit$^+$, sca-1$^+$, and lineage$^-$ (KSL) murine HSCs that are transduced with an simian immunodeficiency virus (SIV)-based lentiviral vector carrying enhanced green fluorescent protein (*eGFP*), driven by a platelet-specific *GPIbα* promoter, enables efficient expression of eGFP in platelets.[4] Because transplantation of KSL cells requires nontransduced bone marrow cells, engraftment by the transduced cells is no >40–55% after transplantation.[4] In order to obviate the need for competitor cells, we validated the transplantation procedure using unfractionated bone marrow cells. As shown in **Figure 1**, transplantation using unfractionated bone marrow cells resulted in more efficient gene targeting to platelets. eGFP expression in platelets was sustained for at least 3 months after transplantation (**Figure 1b**), and we found that 0.60–2.78 vector copies/genome had integrated into the cells of the mice that had received the transplants (**Figure 1c**).

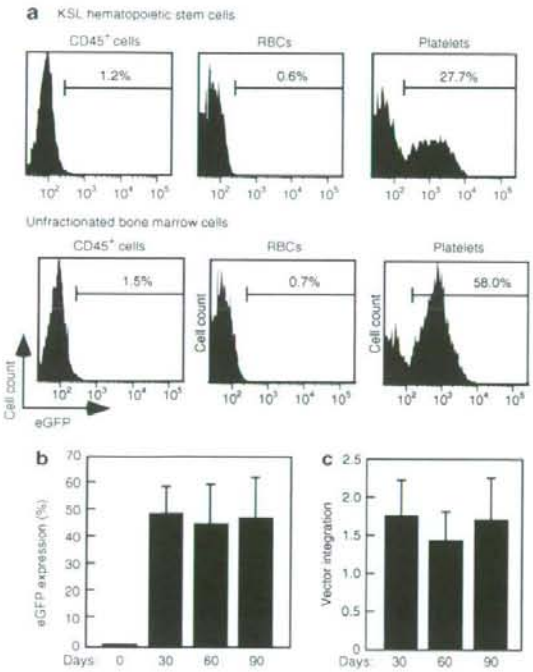

Figure 1 Effects of different stem cell sources on enhanced green fluorescent protein (eGFP) expression in platelets *in vivo*. KSL cells or whole bone marrow cells obtained from Ly5.1 mice were transduced with SIV-GPIbα-eGFP at a multiplicity of infection of 30. Irradiated Ly5.2 mice received either transduced KSL cells (1×10^4) together with competitor cells (2×10^5), or transduced unfractionated bone marrow cells (2×10^6). (**a**) Representative flow cytometry analysis of eGFP-positive cells among CD45$^+$ lymphocytes and granulocytes, red blood cells (RBCs), and platelets in peripheral blood 30 days after transplantation. (**b**) Percentages of eGFP-positive platelets at 30, 60, and 90 days after transplantation. Columns and error bars represent the mean ± SD ($n = 7$). (**c**) Proviral integration into the genomic DNA of bone marrow cells was quantified at 30, 60, and 90 days after transplantation by real-time quantitative PCR. Columns and error bars represent the mean ± SD ($n = 7$). SIV, simian immunodeficiency virus.

hFVII-2RKR expression in platelets induced by platelet-directed gene transduction

The rhFVIIa product currently in clinical use is produced in a single-chain form and activated to the two-chain form during protein purification.[7] Approximately 1% of circulating hFVII in healthy individuals is in the activated form, and the amount of hFVIIa required for bypassing is much larger than the physiological concentration.[7] In order to secrete the activated form of hFVII from transduced cells, we inserted into the factor X activation–cleavage site two arginine/lysine/arginine (RKR) sequences recognized by an intracellular paired basic amino-acid cleaving enzyme/furin type protease, resulting in the secretion of the two-chain molecule with a structure similar to hFVIIa (hFVII-2RKR; **Figure 2a**).[9]

We first examined whether functional FVIIa was produced in megakaryocytes. After transduction with SIV vector containing *hFVII-2RKR* driven by cytomegalovirus promoter, hFVII antigen in the supernatant from the megakaryoblastic cell line UT-7/TPO was detected and found to have activity similar to that from HEP-G2 cells (**Figure 3a** and **c**). The FVII activity of FVII-2RKR was much higher than that of plasma-derived hFVII (**Figure 3c**), thereby suggesting that FVII-2RKR could be cleaved into two chains. In addition, mRNA expression of γ-glutamyl carboxylase, which post-translationally modifies glutamyl residues into γ-carboxyglutamyl residues of vitamin K–dependent coagulation

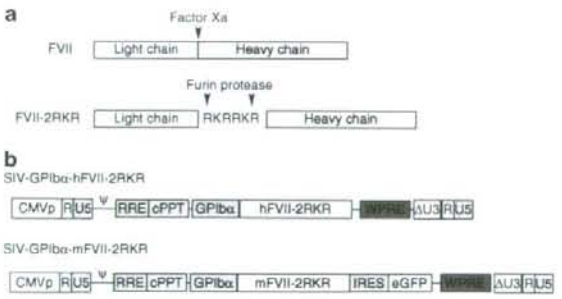

Figure 2 Schematic representation of factor VII (FVII) and simian immunodeficiency virus (SIV) lentiviral vector. (**a**) FVII and engineered activated FVII (FVII-2RKR) construct showing the light and heavy chains. Arrows indicate the recognition sites of physiological factor X activation (FXa) and the intracellular paired basic amino-acid cleaving enzyme/furin type protease. (**b**) The SIV lentiviral vector for platelet-specific gene expression consisted of a cytomegalovirus (CMV)/long-terminal repeat (LTR) chimeric promoter followed by a packaging signal (ψ), a rev-binding element (RRE) for cytoplasmic export of the RNA, the transgene expression region consisting of an internal promoter (*GPIbα*) and the transgene (*hFVII-2RKR* or *mFVII-2RKR-IRES-eGFP*), woodchuck hepatitis virus post regulatory element (WPRE), and a 3′-self-inactivating LTR. cPPT, central polypurine tract; eGFP, enhanced green fluorescent protein; hFVII, human FVII; IRES, internal ribosomal entry site; mFVII, murine FVII.

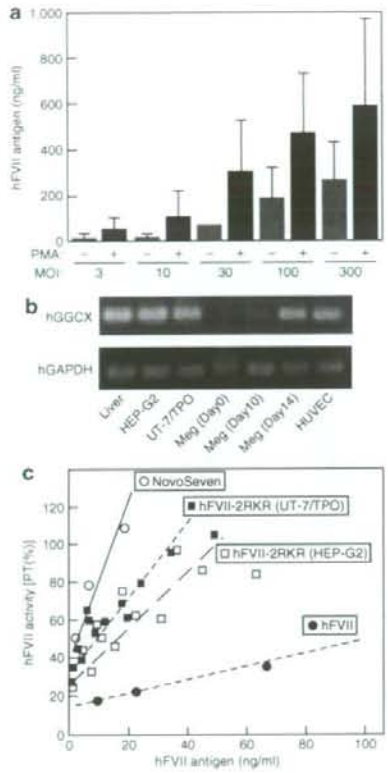

Figure 3 Production of functional hFVII-2RKR by UT-7/TPO cells transduced with simian immunodeficiency virus (SIV) vector. (**a**) UT-7/TPO cells were transduced with SIV-CMV-hFVII-2RKR at the multiplicity of infection (MOI) indicated. hFVII antigen in the supernatant from the cells treated without or with 5 μmol/l phorbol 12-myristate 13-acetate (PMA) for 24 hours were measured using enzyme-linked immunosorbent assay. Columns and error bars represent the mean ± SD (n = 3). (**b**) mRNA expression of γ-glutamyl carboxylase (GGCX) was determined using reverse transcriptase-PCR (RT-PCR). As a control, RT-PCR analysis for human glyceraldehyde 3-phosphate dehydrogenase (GAPDH) transcript was performed simultaneously. (**c**) Comparison between activity and antigen levels of hFVII-2RKR produced by UT-7/TPO and HEP-G2 cells, NovoSeven, and plasma-derived full-length hFVII. CMV, cytomegalovirus; hFVII, human factor VII; HUVEC, human umbilical vein endothelial cells; Meg, CD34$^+$-derived megakaryocytes at days 0, 10, and 14 after the start of differentiation with 10 ng/ml of interleukin-3 and 50 ng/ml of thrombopoietin.

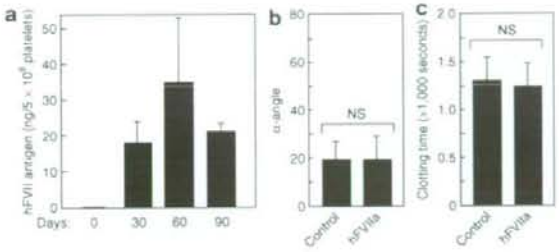

Figure 4 Human factor VII (hFVII) expression in platelets after transplantation of transduced stem cells. FVIII-deficient mice were given transplants of unfractionated bone marrow cells transduced without (control) or with SIV-GPIbα-hFVII-2RKR (hFVIIa). (**a**) Peripheral blood was drawn from the transplant-recipient mice at the indicated times, and the hFVII antigen levels in platelet lysates were measured using enzyme-linked immunosorbent assay. Columns and error bars represent the mean ± SD (n = 4 per group). (**b** and **c**) Whole-blood coagulation was assessed using thromboelastography. Quantitative data of panel **b** α-angle and panel **c** clotting time are shown (n = 7 for control; n = 8 for hFVIIa). Columns and error bars represent the mean ± SEM. Differences between the two groups were analyzed statistically using Student's t-test. NS, not significant. SIV, simian immunodeficiency virus.

factor, was confirmed in megakaryocytes (**Figure 3b**). These data suggest that platelet precursor megakaryocytes efficiently produce functional FVIIa after transduction.

We next examined whether transduction of HSCs enabled FVIIa expression in platelets. For this purpose, hFVII was used to discriminate transduced FVII from endogenous mFVII. An SIV vector equipped with *hFVII-2RKR* driven by *GPIbα* promoter was created (**Figure 2b**) and used for infecting unfractionated bone marrow cells. After transplantation of the transduced cells into lethally irradiated FVIII-deficient mice, hFVII antigen levels were detected in platelet lysates for at least 90 days (**Figure 4a**). Importantly, hFVII antigen was not detected in the plasma even after stimulation of the platelets with collagen and phorbol 12-myristate 13-acetate (data not shown); therefore, we did not assay for FVII activity in plasma.

We next examined the improvement of whole-blood coagulation in the transplant-recipient mice. The conventional activated partial thromboplastin time, a useful marker for gene therapy in mouse models of hemophilia, did not seem to reflect the phenotypic correction directly, as seen from the fact that platelet-derived hFVII antigen could not be detected in plasma. Therefore we employed thromboelastography (TEG) to record the continuous profile of whole-blood coagulation.[10] TEG can be used for evaluating the effects of hemostatic agents such as rhFVIIa,[11] and to assess the effects of different pharmacological interventions on various factors (coagulation, platelet activation, and platelet–fibrin interaction) involved in clot formation. As shown in **Figure 4b** and **c**, whole-blood coagulation in FVIII-deficient mice, as assessed by TEG, did not improve after transplantation. The mortality rate after tail clipping was not altered by transplantation (data not shown).

In order to investigate why phenotypic correction was not observed after transplantation, we validated the expression and localization of hFVII by immunogold electron microscopy. We confirmed that hFVII antigen was abundant in cytoplasm of platelets obtained from transplant-recipient mice (**Figure 5a**). When platelets were stimulated with phorbol 12-myristate 13-acetate, most of the hFVII antigen was redistributed to the sub-membrane zone, and was partly expressed on the surface (**Figure 5b**). These data confirmed that hFVII is efficiently stored in platelets after transplantation of transduced bone marrow cells, and is expressed on the cell surface after platelet activation.

Phenotype correction of FVIII-deficient mice by expression of mFVII-2RKR in platelets

We hypothesized that the failure of hFVII-2RKR expression in platelets may be because of inefficient interaction of hFVII-2RKR with murine TF.[12,13] Indeed, higher concentrations of rhFVIIa (NovoSeven; ≥20 μg/ml) were required to restore coagulation in

FVIII-deficient mice (data not shown). We therefore generated an mFVII construct in an analogous fashion (mFVII-2RKR) to further prove its efficacy in FVIII-deficient mice (**Figure 2b**). Because we could not create an enzyme-linked immunosorbent assay for mFVII antigen, an *eGFP* gene driven by the internal ribosomal entry site was inserted just after the *mFVII-2RKR* gene to give indirect confirmation of mFVII-2RKR expression in platelets (**Figure 2b**). Although eGFP expression in platelets after transplantation was limited to 3–12% of the platelets, the pattern of eGFP expression under the control of the internal ribosomal entry site sequence was much weaker than that driven directly by the upstream promoter (data not shown). It appears, therefore, that the levels of ectopically expressed mFVII-2RKR in platelets are much higher than would be expected from the results of eGFP expression. This reasoning was supported by the results of proviral integration into the genome (1.15 ± 2.42; $n = 13$), which were similar to those obtained from mice expressing eGFP in 28.6–74.3% of platelets by transduction with SIV-GPIbα-eGFP (see **Figure 1c**).

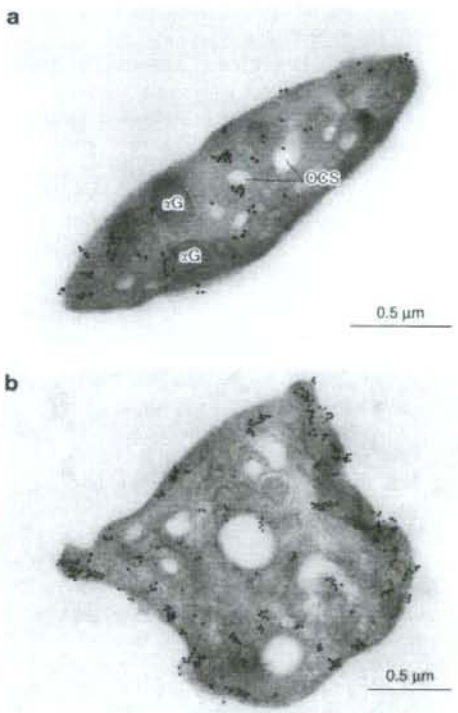

Figure 5 Immunoelectron microscopic localization of ectopically expressed hFVII-2RKR in platelets. FVIII-deficient mice were given transplants of unfractionated bone marrow cells transduced with SIV-GPIbα-hFVII-2RKR. Isolated platelets from the transplant-recipient mice were stimulated (**a**) without or (**b**) with 100 nmol/l phorbol 12-myristate 13-acetate for 15 minutes. Cells were incubated with a biotin-labeled rabbit anti-hFVII antibody. Bound antibodies were detected using a colloidal gold–conjugated goat anti-biotin secondary antibody. hFVII expression in platelets was examined by electron microscopy. αG, α-granule; hFVII, human factor VII; OCS, open canalicular system; SIV, simian immunodeficiency virus.

In comparison with the results obtained from hFVII-2RKR, whole-blood coagulation, as assessed by TEG, was significantly improved in mice that had received the transplant (**Figure 6a**). The α-angle, which represents the rate of clot formation, was enhanced (**Figure 6b**), and the clotting time was significantly shortened

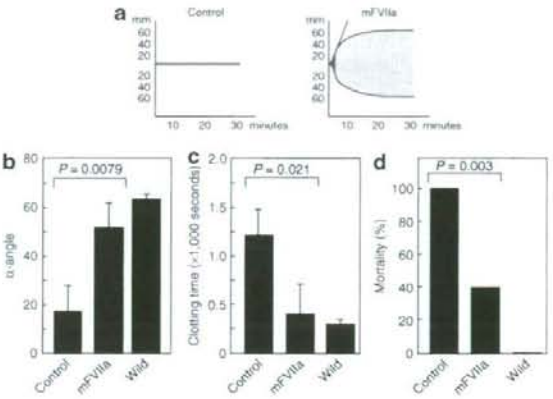

Figure 6 Phenotype correction of factor VIII (FVIII)-deficient mice by ectopic expression of mFVII-2RKR in platelets. FVIII-deficient mice were given transplants of unfractionated bone marrow cells transduced without (control) or with SIV-GPIbα-mFVII-2RKR (mFVIIa). (**a**) Representative thromboelastography data obtained from control and mFVII-2RKR-transfected mice. (**b** and **c**) Quantitative data of panel **b** α-angle and panel **c** clotting time are shown ($n = 8$ for control; $n = 8$ for mFVIIa). The data obtained from wild-type mice are also shown ($n = 6$). Columns and error bars represent the mean ± SEM. Differences between the two groups were analyzed statistically using Student's *t*-test. (**d**) Mortality rates within 24 hours of tail clipping in wild-type mice ($n = 6$) or FVIII-deficient mice given transplants of control or SIV-GPIbα-mFVII-2RKR-transduced bone marrow cells ($n = 10$ for control; $n = 10$ for mFVIIa). The mortality rate was analyzed statistically using the χ^2-test. mFVIIa, murine activated factor VII; SIV, simian immunodeficiency virus.

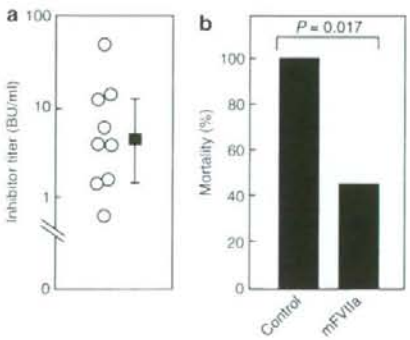

Figure 7 Effects of mFVII-2RKR expression in platelets on phenotypic correction in factor VIII (FVIII)-deficient mice in the presence of anti-FVIII inhibitors. (**a**) Circulating inhibitors were detected in 9 of the 13 FVIII-deficient mice after peritoneal injection of recombinant hFVIII. (**b**) In the presence of circulating inhibitors, mortality ratio at 24 hours after tail clipping was examined in FVIII-deficient mice given transplants of control or SIV-GPIbα-mFVII-2RKR-transduced bone marrow cells [$n = 10$ for control; $n = 9$ for mFVII-2RKR (mFVIIa)]. The mortality rate was analyzed statistically using the χ^2-test. mFVIIa, murine activated factor VII; SIV, simian immunodeficiency virus.

(**Figure 6c**). The mortality rate after tail clipping was significantly reduced in mice with transplants (**Figure 6d**). In addition, five of the nine FVIII-deficient mice that received bone marrow cells transduced with SIV-GPIbα-mFVII-2RKR survived after tail clipping despite the presence of circulating inhibitors against hFVIII (**Figure 7a** and **b**). Blood coagulation, as assessed by TEG, was similarly corrected in FVIII-deficient mice having FVIII-neutralizing inhibitors, by treating them with SIV-GPIbα-mFVII-2RKR (data not shown). Taking these results together, platelet-specific mFVII-2RKR expression results in efficient bypass therapy to activate factor X activation, thereby resulting in thrombin generation on platelet surfaces in FVIII-deficient mice.

DISCUSSION

Hemophilia is considered to be a suitable condition for gene therapy because it is caused by a single gene abnormality, and therapeutic coagulation factor levels may vary across a broad range (5–100%).[14] Although sustained therapeutic expression of FVIII has been achieved in preclinical studies using a wide range of gene transfer technologies targeted at different tissues, the emergence of neutralizing antibodies often limits the clinical applications.[15] Blood platelets have been receiving much attention as novel target cells for hemophilia gene therapy, because platelet-specific expression of FVIII abolishes the emergence of neutralizing antibodies, and platelet-derived FVIII supports hemostasis in the presence of high titers of FVIII-neutralizing antibodies.[2–5] Here, we extended the application of platelet-directed gene therapy to demonstrate that FVII-2RKR expression in platelets improved the bleeding phenotype of FVIII-deficient mice, even in the presence of FVIII-neutralizing antibodies. Given that rhFVIIa has proven efficacy in the treatment of hemophilia patients with the inhibitors,[8] platelets expressing FVII-2RKR may be a potential alternative to bolus administration of rhFVIIa in such patients.

It is possible that platelets store ectopically expressed FVII-2RKR in the cytoplasm, and that this is specifically expressed on the cell surface after activation. Although hFVII antigen levels achieved here seemed to be much lower than the therapeutic level, whole-blood clotting, as assessed by TEG, and mortality rate after tail clipping were significantly improved when mFVII-2RKR was expressed. These data suggest that FVII-2RKR in platelets can locally generate a thrombin burst at the site of vascular injury. Although an important drawback of rhFVIIa administration is its short half-life (2.6–2.8 hours), which necessitates frequent bolus injections to stop bleeding,[7,16] platelets may be able to store stable FVII-2RKR in the circulation. The importance of coagulation factor stored in platelets is supported by the role of platelet factor V in hemostasis. Platelet-derived platelet factor V appears to support hemostasis even in patients with an acquired platelet factor V inhibitor, thereby suggesting that platelets can deliver coagulation factors and protect them from being degraded by platelet factor V inhibitors.[17] Recently, erythroid-specific factor IX expression, driven by the *β-globin* promoter, has been shown to result in phenotypic correction of hemophilia B in mice.[18] However, given the context of the specific release or expression of a target protein at the site of thrombus formation, platelet-directed gene therapy has an advantage as a therapy for inherited coagulation factor deficiencies.

Contrary to our initial expectations, the sub-localization of ectopically expressed hFVII-2RKR in platelets is quite different from that described in previous reports of FVIII expression.[3,19] Retroviral transduction of FVIII in human $CD34^+$ HSCs enables FVIII-transduced megakaryocytes to store human FVIII with von Willebrand factor, a natural carrier protein of FVIII, within α-granules.[19] In this study, hFVII-2RKR was found to be localized in the cytoplasm, but not in α-granules, suggesting that storage of this ectopically expressed protein in α-granules requires specific binding with an endogenous protein, as is the case for the FVIII–von Willebrand factor interaction.[20] Despite the failure to localize in α-granules, cytoplasmic hFVII-2RKR translocated to a sub-membrane fraction and was expressed on the cell surface after platelet activation. It is possible that activated platelets can express FVII-2RKR through a mechanism of protein secretion other than granule release. Phosphatidylserine flip-flop is one candidate that may be responsible for the surface expression of FVII-2RKR; however, we do not yet have a clear explanation for this. Recently, it has been reported that platelets supply their own TF for thrombin generation in a temporally and spatially circumscribed process.[21,22] This would suggest that TF expression in platelets is involved in the hemostatic function of ectopically expressed FVII-2RKR, even in the absence of soluble TF. The failure of hFVII-2RKR expression in platelets to correct the bleeding phenotype, in contrast to mFVII-2RKR, further demonstrates the TF-dependence of coagulation mediated by platelet-derived FVIIa; murine TF appears to be more species-specific and interacts poorly with hFVIIa.[12,13]

Before proceeding to further clinical application, we should weigh the clinical benefits and risks of FVII-2RKR expression in platelets. The most important drawback of FVIIa expression is a potential risk for thromboembolic events. In this study, the clinical effect of FVII-2RKR expression seemed to be less than that of FVIII expression in platelets. Although a correction of as little as 1% of FVIII in platelets was reportedly enough to cure FVIII-null mice,[3–5] our strategy resulted only in a partial cure in the current model. One explanation of the lower efficacy is that much higher expression of FVII-2RKR is needed to generate sufficient thrombin in FVIII-deficient mice. We will need to further improve the transduction efficiency and modify the enzymatic activity of FVIIa. We believe that megakaryocyte- and platelet-specific expression of FVIIa in targeting HSCs is important for safety, given that expression of FVIIa in neutrophils or monocytes may alter the coagulation properties of blood cells, leading to an unexpected thrombosis similar to disseminated intravascular coagulation. Once the approach involving the targeting of platelets has been optimized for greater efficacy, it is possible that the risk of unexpected thrombosis will become a major concern. Further, we must consider the risk of insertional mutagenesis of the integrating vector. While lentiviral vectors offer a means to correct genetic diseases by integration into chromosomal DNA permanently, all the integrating gene transfer vectors in current use carry a risk of insertional mutagenesis.[23] In view of the fact that the target diseases for platelet-directed gene therapy, including hemophilia, are not generally lethal disorders, we have to continue investigating the safety of platelet-directed gene therapy using integrating vectors to the maximum. Observations should be carried on for extended durations in order

to substantiate long-term *in vivo* gene expression and vector safety. Our observations were limited to 3 months.

In this study, we demonstrated that FVII-2RKR expression in platelets by SIV vectors could be an important strategy for treating hemophilia A. Given that platelets play a central role and provide the scaffolding for the coagulation cascade, this would be a reasonable approach, similar to the proven therapeutic effects of rhFVIIa infusion, for treating a number of hemorrhagic diseases, such as hemophilia, Glanzmann's thrombasthenia, and FVII deficiency. Further evaluations utilizing larger animals such as Cynomolgus monkeys or dogs will be necessary to determine efficient and safe protocols for platelet-directed gene therapy.

MATERIALS AND METHODS

The materials and methods for cell culture, reverse transcriptase-PCR, proviral integration, mouse blood preparation, enzyme-linked immunosorbent assay for hFVII antigen, determination of hFVII activity, and flow cytometry are described in the **Supplementary Materials and Methods**.

Plasmid constructs and production of SIV lentiviruses. The methods for cDNA cloning and plasmid construction are described in detail in **Supplementary Materials and Methods**. A self-inactivating SIV vector plasmid was generated as described earlier (**Figure 1b**).[24] SIV lentiviral vectors were produced as described earlier.[4] Briefly, the SIV vector and each packaging vector (*gag/pol*, *rev*, and *VSV-G*) were co-transfected into HEK293T cells using the Lipofectamine PLUS reagent (Invitrogen, Carlsbad, CA). The supernatants were collected 48 hours after transfection and filtered through a 0.4-μm filter. The transduction units of the lentiviral vector and proviral integration into the genomic DNA were measured as described earlier.[4]

Isolation of KSL cells, viral transduction, and stem cell transplantation. Mice with FVIII-deficient hemophilia A with targeted destruction of exon 16 of the *FVIII* gene were kindly provided by Dr H.H. Kazazian Jr. (University of Pennsylvania, Philadelphia, PA). C57BL/6 (Ly5.2) mice were purchased from Japan SLC (Shizuoka, Japan). C57BL/6 mice congenic for the Ly5 locus (Ly5.1) were purchased from Sankyo-Lab Service (Tokyo, Japan). All animal procedures were approved by the Institutional Animal Care and Concern Committee at Jichi Medical University (Tochigi, Japan), and animal care was in accordance with the committee's guidelines.

KSL HSCs were isolated as described earlier.[4] KSL cells or unfractionated bone marrow cells were precultured for 24 hours before viral transduction in Stem Pro Medium (Invitrogen, Carlsbad, CA) supplemented with 100 ng/ml stem cell factor, 10 ng/ml thrombopoietin, 100 ng/ml interleukin-6, 100 ng/ml Flt-3 ligand, and 400 ng/ml soluble interleukin-6 receptor. The cells were transduced with SIV vectors at a multiplicity of infection of 30 in the presence of the same cytokine combination, and incubated at 37 °C for 12 hours. The recipient mice (Ly5.2 mice or FVIII-deficient mice at 8–12 weeks of age) were irradiated with a single lethal dose of 9.5 Gy (Gamma Cell; Norton International, Ontario, Canada), and then administered either transduced KSL cells (1×10^4) and Ly5.2 competitor cells (2×10^5), or transduced whole bone marrow cells (2×10^6). The methods for transduction of UT-7/TPO and HEP-G2 cells by SIV vector are described in **Supplementary Materials and Methods**.

Immunogold electron microscopy. Washed murine platelets were obtained as described earlier.[25] The resting and phorbol 12-myristate 13-acetate–stimulated platelets were fixed in 0.1% glutaraldehyde in 0.1 mol/l phosphate buffer (pH 7.4) at 4 °C for 1 hour. The fixed platelets were transferred into Eppendorf tubes, centrifuged at 3,000 rpm for 3 minutes, and rinsed with phosphate-buffered saline five times at 4 °C. The specimens were sequentially immersed in 1 mol/l sucrose in phosphate-buffered saline for 1 hour, and then in 1.84 mol/l sucrose containing 20% polyvinylpyrrolidone (Sigma-Aldrich, St. Louis, MO) in phosphate-buffered saline overnight at 4 °C.[26] The specimens were frozen in liquid nitrogen and ultra-thin frozen sections were prepared, incubated with biotin-labeled rabbit anti-hFVII antibody, washed with phosphate-buffered saline, and then incubated with goat anti-biotin antibody coupled to 15 colloidal gold (BBI International, Cardiff, UK). After being stained with uranyl acetate, the sections were examined using a JEM-1200EX electron microscope (JEOL, Tokyo, Japan) at an acceleration voltage of 80 kV.

TEG and tail clipping. The principle of TEG is based on measurement of the physical viscoelastic characteristics of blood clots. Whole blood for TEG was drawn at 30–60 days after transplantation. Clot formation was monitored in whole blood at 37 °C, in an oscillating plastic cylindrical cuvette having a coaxially suspended stationary piston with 1-mm clearance between the surfaces, using a computerized TEG (ROTEG; Pentapharm, Munich, Germany). A sample (270 μl) of whole blood was carefully drawn from the superior vena cava of anesthetized mice using a syringe containing 30 μl sodium citrate. Whole-blood coagulation was initiated with the addition of 20 μl of 200 mmol/l $CaCl_2$, and TEG was used to assess the coagulation by measuring various parameters, such as the latency for clotting time, and the kinetics of clot development, as determined by the α-angle.[10] When blood coagulation was not observed within 30 minutes, the clotting time and α-angle were defined as 1,800 seconds and 0°, respectively. Phenotypic correction was tested in some of the transplant-recipient mice by anesthetizing them with diethyl ether and clipping 1.0 cm off the ends of their tails. The mice were then observed for 24 hours to determine the rate of mortality.

Circulating FVIII inhibitors. Antibodies against hFVIII were produced by administering weekly peritoneal injections of 0.05 U/g body weight of rhFVIII (Kogenate FS; Bayer AG, Wuppertal, Germany). In view of the possibility that lethal irradiation could cancel the circulating anti-FVIII antibodies (data not shown), we started immunization with hFVIII 1 month after transplantating bone marrow cells transduced with SIV-GPIbα-mFVII-2RKR. Analysis of neutralizing antibodies against hFVIII was performed using the Bethesda method described earlier.[27] After five immunizations, we could detect circulating inhibitors against hFVIII, as assessed in Bethesda units (**Figure 7a**).

SUPPLEMENTARY MATERIAL

Materials and Methods.

ACKNOWLEDGMENTS

We are deeply grateful to Naoko Matsumoto and Masanori Ito for their excellent technical assistance. We are also grateful to H.H. Kazazian Jr. (University of Pennsylvania, Philadelphia, PA) for providing the FVIII-deficient mice, and N. Komatsu (Yamanashi University, Yamanashi, Japan) for UT-7/TPO. This work was supported by grants from the Mitsubishi Pharma Research Foundation (to T.O.), Grants-in-aid for Scientific Research from the Ministry of Education and Science (19591133 to S.M. and 18591084 to J.M.), Health and Labour Science Research Grants for Research from the Ministry of Health, Labour and Welfare (H17-nanchi-ippan-002 and H18-eizu-ippan-003 to Y.S.), and grants for "High-Tech Center Research" Projects for Private Universities with matching fund subsidies from MEXT (Ministry of Education, Culture, Sports, Science and Technology), 2002–2006 (to Y.S).

REFERENCES

1. Kufrin, D, Eslin, DE, Bdeir, K, Murciano, JC, Kuo, A, Kowalska, MA *et al.* (2003). Antithrombotic thrombocytes: ectopic expression of urokinase-type plasminogen activator in platelets. *Blood* **102**: 926–933.
2. Yarovoi, HV, Kufrin, D, Eslin, DE, Thornton, MA, Haberichter, SL, Shi, Q *et al.* (2003). Factor VIII ectopically expressed in platelets: efficacy in hemophilia A treatment. *Blood* **102**: 4006–4013.
3. Shi, Q, Wilcox, DA, Fahs, SA, Weiler, H, Wells, CW, Cooley, BC *et al.* (2006). Factor VIII ectopically targeted to platelets is therapeutic in hemophilia A with high-titer inhibitory antibodies. *J Clin Invest* **116**: 1974–1982.
4. Ohmori, T, Mimuro, J, Takano, K, Madoiwa, S, Kashiwakura, Y, Ishiwata, A, *et al.* (2006). Efficient expression of a transgene in platelets using simian immunodeficiency

virus-based vector harboring glycoprotein Ibalpha promoter: *in vivo* model for platelet-targeting gene therapy. *FASEB J* **20**: 1522–1524.
5. Shi, Q, Wilcox, DA, Fahs, SA, Fang, J, Johnson, BD, Du, LM *et al.* (2007). Lentivirus-mediated platelet-derived factor VIII gene therapy in murine haemophilia A. *J Thromb Haemost* **5**: 352–361.
6. Mackman, N, Tilley, RE and Key, NS (2007). Role of the extrinsic pathway of blood coagulation in hemostasis and thrombosis. *Arterioscler Thromb Vasc Biol* **27**: 1687–1693.
7. Jurlander, B, Thim, L, Klausen, NK, Persson, E, Kjalke, M, Rexen, P *et al.* (2001). Recombinant activated factor VII (rFVIIa): characterization, manufacturing, and clinical development. *Semin Thromb Hemost* **27**: 373–384.
8. Franchini, M, Zaffanello, M and Veneri, D (2005). Recombinant factor VIIa. An update on its clinical use. *Thromb Haemost* **93**: 1027–1035.
9. Margaritis, P, Arruda, VR, Aljamali, M, Camire, RM, Schlachterman, A and High, KA (2004). Novel therapeutic approach for hemophilia using gene delivery of an engineered secreted activated factor VII. *J Clin Invest* **113**: 1025–1031.
10. Luddington, RJ (2005). Thrombelastography/thromboelastometry. *Clin Lab Haematol* **27**: 81–90.
11. Sørensen, B and Ingerslev, J (2004). Thromboelastography and recombinant factor VIIa-hemophilia and beyond. *Semin Hematol* **41(suppl. 1)**: 140–144.
12. Janson, TL, Stormorken, H and Prydz, H (1984). Species specificity of tissue thromboplastin. *Haemostasis* **14**: 440–444.
13. Nelsestuen, GL, Stone, M, Martinez, MB, Harvey, SB, Foster, D and Kisiel, W (2001). Elevated function of blood clotting factor VIIa mutants that have enhanced affinity for membranes. Behavior in a diffusion-limited reaction. *J Biol Chem* **276**: 39825–39831.
14. Lozier, J (2004). Gene therapy of the hemophilias. *Semin Hematol* **41**: 287–296.
15. High, K (2005). Gene transfer for hemophilia: can therapeutic efficacy in large animals be safely translated to patients? *J Thromb Haemost* **3**: 1682–1691.
16. Hedner, U (2001). Recombinant factor VIIa (Novoseven) as a hemostatic agent. *Semin Hematol* **38**(suppl. 12): 43–47.
17. Perdekamp, MT, Rubenstein, DA, Jesty, J and Hultin, MB (2006). Platelet factor V supports hemostasis in a patient with an acquired factor V inhibitor, as shown by prothrombinase and tenase assays. *Blood Coagul Fibrinolysis* **17**: 593–597.
18. Chang, AH, Stephan, MT and Sadelain, M (2006). Stem cell-derived erythroid cells mediate long-term systemic protein delivery. *Nat Biotechnol* **24**: 1017–1021.
19. Wilcox, DA, Shi, Q, Nurden, P, Haberichter, SL, Rosenberg, JB, Johnson, BD *et al.* (2003). Induction of megakaryocytes to synthesize and store a releasable pool of human factor VIII. *J Thromb Haemost* **1**: 2477–2489.
20. Federici, AB (2003). The factor VIII/von Willebrand factor complex: basic and clinical issues. *Haematologica* **88**: EREP02.
21. Panes, O, Matus, V, Saez, CG, Quiroga, T, Pereira, J and Mezzano, D (2007). Human platelets synthesize and express functional tissue factor. *Blood* **109**: 5242–5250.
22. Schwertz, H, Tolley, ND, Foulks, JM, Denis, MM, Risenmay, BW, Buerke, M *et al.* (2006). Signal-dependent splicing of tissue factor pre-mRNA modulates the thrombogenicity of human platelets. *J Exp Med* **203**: 2433–2440.
23. Nienhuis, AW, Dunbar, CE and Sorrentino, BP (2006). Genotoxicity of retroviral integration in hematopoietic cells. *Mol Ther* **13**: 1031–1049.
24. Nakajima, T, Nakamaru, K, Ido, E, Terao, K, Hayami, M and Hasegawa, M (2000). Development of novel simian immunodeficiency virus vectors carrying a dual gene expression system. *Hum Gene Ther* **11**: 1863–1874.
25. Leng, XH, Hong, SY, Larrucea, S, Zhang, W, Li, TT, López, JA *et al.* (2004). Platelets of female mice are intrinsically more sensitive to agonists than are platelets of males. *Arterioscler Thromb Vasc Biol* **24**: 376–381.
26. Suzuki, H, Murasaki, K, Kodama, K and Takayama, H (2003). Intracellular localization of glycoprotein VI in human platelets and its surface expression upon activation. *Br J Haematol* **121**: 904–912.
27. Madoiwa, S, Yamauchi, T, Hakamata, Y, Kobayashi, E, Arai, M, Sugo, T *et al.* (2004). Induction of immune tolerance by neonatal intravenous injection of human factor VIII in murine hemophilia A. *J Thromb Haemost* **2**: 754–762.

European Heart Journal (2008) 29, 1729–1738
doi:10.1093/eurheartj/ehn027

Determinants of thrombin generation, fibrinolytic activity, and endothelial dysfunction in patients on dual antiplatelet therapy: involvement of factors other than platelet aggregability in Virchow's triad

Yuichiro Yano[1], Tsukasa Ohmori[2]*, Satoshi Hoshide[1], Seiji Madoiwa[2], Keiji Yamamoto[1], Takaaki Katsuki[1], Takeshi Mitsuhashi[1], Jun Mimuro[2], Kazuyuki Shimada[1], Kazuomi Kario[1], and Yoichi Sakata[2]

[1]Division of Cardiovascular Medicine, Department of Medicine, Jichi Medical University School of Medicine, 3311-1 Yakushiji, Shimotsuke, Tochigi 329-0498, Japan; [2]Research Division of Cell and Molecular Medicine, Center for Molecular Medicine, Jichi Medical University School of Medicine, 3311-1 Yakushiji, Shimotsuke, Tochigi 329-0498, Japan

Received 4 October 2007; revised 27 December 2007; accepted 10 January 2008; online publish-ahead-of-print 12 February 2008

See page 1699 for the editorial comment on this article (doi:10.1093/eurheartj/ehn257)

Aims	The aim of the study was to assess mechanisms and clinical backgrounds in order to determine residual platelet aggregability in dual antiplatelet therapy and to ascertain whether platelet aggregability is involved in systemic thrombogenicity.
Methods and results	A cross-sectional study was conducted in 85 consecutive patients who underwent dual antiplatelet therapy (aspirin and thienopyridine/cilostazol) after percutaneous coronary intervention (PCI). Although serum thromboxane B_2 and dephosphorylation of vasodilator-stimulated phosphoprotein were significantly abolished, the platelet aggregation tests showed inter-individual differences that could be partly explained by plasma glucose levels. Platelet aggregability was not related to other factors involved in thrombogenicity. Thrombin generation assessed by soluble fibrin was independently associated with total cholesterol ($\beta = 0.349$, $P < 0.001$), brain natriuretic peptide ($\beta = 0.222$, $P = 0.018$), and ankle-brachial index ($\beta = -0.330$, $P = 0.001$). Plasminogen activator inhibitor-1 was associated with the apnea–hypopnea index ($\beta = 0.300$, $P = 0.006$). E-selectin was correlated with diabetes mellitus ($\beta = 0.279$, $P = 0.008$) and body mass index ($\beta = 0.323$, $P = 0.002$).
Conclusion	Although dual antiplatelet therapy effectively inhibited its pharmacological targets, thrombin generation, inhibition of fibrinolytic activity, and endothelial dysfunction were determined by other clinical backgrounds. Our data suggested that some patients remain at risk of thrombotic complications after PCI and that these may benefit from anticoagulant treatment despite adequate dual antiplatelet therapy.

Keywords Percutaneous coronary intervention • Aspirin • Thienopyridine • Antiplatelet drug resistance • Thrombin generation

Introduction

Platelet aggregation plays a central role in the development of thrombotic complications after percutaneous coronary intervention (PCI).[1–3] The role of aspirin in secondary prevention of ischaemic cardiovascular diseases is universally accepted. Furthermore, dual antiplatelet therapy of aspirin combined with thienopyridine (and/or cilostazol) including clopidogrel or

*Corresponding author. Tel: +81 285 58 7397, Fax: +81 285 44 7817, Email: tohmori@jichi.ac.jp

ticlopidine is the gold standard for preventing major cardiovascular events in patients undergoing PCI, especially since the beginning of the balloon-expandable stent era.[4–6] In contrast, nearly 20% of patients continue to have further cardiovascular events after PCI, despite the superior protection conferred by dual antiplatelet therapy, as shown in a number of clinical trials.[7]

The mechanism by which antiplatelet therapy fails in certain patients after PCI, in part, thought to be attributed to the fact that some individuals have impaired antiplatelet responses, is referred to as 'aspirin resistance' or 'clopidogrel resistance'.[8–10] There is evidence that not all patients respond comparably to antiplatelet drugs, as evaluated by non-specific laboratory test such as aggregometry, and hence the concept of drug 'resistance' has arisen.[11–14] However, recent evidence suggest that when the definition of resistance is limited to situations in which the drugs fail to hit their pharmacological targets, resistance against antiplatelet drug appears to be rare.[15–18] Many published studies of antiplatelet resistance have been carried out using nonspecific platelet aggregation tests, which merely identify patients on antiplatelet therapy with high residual platelet activation.[7,18] Despite this drawback, identification of patients with high residual platelet reactivity may be useful for predicting individuals risks of atherothrombotic events.[7–10,13,17]

The results of clinical trials on the use of anticoagulant agents and the involvement of fibrin fibrils and inflammatory cells in the formation of occlusive thrombi suggest that not only platelets but also the coagulation cascade, fibrinolytic system, inflammation, and endothelial dysfunction may orchestrate *in vivo* thrombus formation, thereby leading to clinical treatment failure under dual antiplatelet therapy.[19–21] Indeed, the clinical outcomes of patients undergoing PCI were reported to be associated with the levels of D-dimer, plasminogen activator inhibitor-1 (PAI-1), E-selectin, and markers for thrombin generation.[22–25] However, there is no sufficient data that correlate heightened platelet reactivity during dual antiplatelet therapy with other markers for coagulation, fibrinolysis, and endothelial dysfunction. The aims of the present study were to assess the various clinical backgrounds associated with high residual platelet aggregability under dual antiplatelet therapy and to clarify any association with thrombin generation, fibrinolytic activity, and endothelial dysfunction that might lead to clinical failure against antiplatelet therapy.

Methods

Patients and study protocol

The institutional review board at the Jichi Medical University approved the study protocols, and written informed consent was obtained from all participants. We enrolled consecutive hospitalized patients from July 2006 to April 2007 who were treated by PCI because of symptomatic coronary artery disease, including unstable angina, and non-ST-elevation or ST-elevation myocardial infarction. We estimated the sample size required using a general formula for the correlation coefficient.[26] We set $\alpha = 0.05$, $\beta = 0.20$, and expected a correlation coefficient, $r = 0.30–0.35$. Using the formula, at least 62–85 participants would be required for the study. All patients had taken dual antiplatelet therapy, consisting of 100 mg/day of aspirin and 200 mg/day of ticlopidine, 75 mg/day of clopidogrel, or 200 mg/day of cilostazol (*Table 1*). The exclusion criteria were as follows: acute coronary syndrome within 10 days; New York Heart Association Class III or IV heart failure; ingestion of other drugs affecting platelet function or coagulation; platelet counts of $<10\times10^7$ or $>40\times10^7$ ml^{-1}; myeloproliferative disorders; autoimmune diseases; malignant diseases; and atrial fibrillation. Compliance with antiplatelet drugs was determined by nursing staff during hospitalization. After normalization of cardiac enzymes (just before discharge), patients underwent blood sampling, ambulatory blood pressure monitoring (ABPM; TM-2425; A&D Co., Inc., Tokyo, Japan), ankle-brachial index (ABI) monitoring (FORM/ABI; Colin Co. Ltd., Ehime, Japan), and cardiorespiratory monitoring (Somte; Compumedics, Melbourne, Australia).

Table 1 Characteristics of the study population

Variables	Total subjects ($n = 85$)
Age (years)	60.0 ± 13.1
Men, *n* (%)	70 (82)
Body mass index (kg/m^2)	24.3 ± 3.3
Current smoker, *n* (%)	50 (59)
Family history of coronary artery disease, *n* (%)	26 (31)
Hypertension, *n* (%)	59 (69)
Diabetes mellitus, *n* (%)	36 (42)
Dyslipidemia, *n* (%)	75 (88)
Prior myocardial infarction, *n* (%)	10 (12)
Presenting symptoms, *n* (%)	
Unstable angina	22 (26)
Myocardial infarction	63 (74)
Coronary artery disease, *n* (%)	
One-vessel disease	41 (48)
Two-vessel disease	26 (31)
Three-vessel disease	18 (21)
Concomitant medications	
Antiplatelet agents, *n* (%)	
Aspirin	85 (100)
Ticlopidine	72 (85)
Clopidogrel	3 (4)
Cilostazol	10 (12)
Antihypertensive medication, *n* (%)	
Beta blocker	51 (60)
Angiotensin-converting enzyme inhibitor	39 (46)
Angiotensin II receptor blocker	32 (38)
Calcium channel blocker	17 (20)
Diuretic	14 (16)
Nitrate, *n* (%)	5 (6)
Statin, *n* (%)	66 (78)
Proton pump inhibitor, *n* (%)	1 (1)
Non-steroidal anti-inflammatory drug, *n* (%)	0 (0)

Data for continuous variables are expressed as the mean ± SD.

To assess the effects of antiplatelet therapy, 20 healthy individuals who were not taking any antiplatelet drugs were enrolled as controls.

Platelet aggregation

A fasting venous sample was carefully collected via a 21-gauge needle into a syringe containing 1/10 volume of sodium citrate between 07:30 and 08:00 h. Platelet-rich plasma (PRP) was obtained by centrifuging whole blood at 200 g for 12 min. The time from blood collection to measurement was standardized to 1 h. The aggregation response was measured based on the light scattering intensities obtained with a PA-200 Platelet Aggregation Analyzer (Kowa Co. Ltd., Tokyo, Japan).[27] This device is particularly sensitive for detecting the sizes of small platelet aggregates.[27,28] Platelet aggregation was performed without any agonists, or with collagen (Hormon-Chemie, Munich, Germany), adenosine diphosphate (ADP) (MC Medical Co., Tokyo, Japan), and thrombin receptor-activating peptide (TRAP; Invitrogen Co., Carlsbad, CA, USA), a specific agonist for protease-activating receptor-1. Spontaneous small platelet aggregation was defined by small aggregate formation by stirring without agonist.

Phosphorylation of vasodilator-stimulated phosphoprotein in platelets

Phosphorylation of vasodilator-stimulated phosphoprotein (VASP) is regulated by the cAMP level, which is thus believed to be a marker of $P2Y_{12}$ receptor reactivity.[29] To determine the VASP phosphorylation state of whole blood, we used a standardized flow cytometric assay (PLT VASP/P2Y12; Biocytex, Marseille, France) with some modifications. We found that the commercially available VASP phosphorylation assay appeared to contain an extremely high concentration of ADP. In our protocol, cAMP elevation by 1 μM PGI_2 increased the VASP phosphorylation level by stimulation of adenylate cyclase. When simultaneously stimulated with 2 μM ADP, the signaling from G_i activation mediated via $P2Y_{12}$ reduced the phosphorylation of VASP induced by PGI_2. However, when the $P2Y_{12}$ receptor was successfully inhibited by active metabolites of thienopyridines, or phosphodiesterase that was inhibited by cilostazol, ADP was unable to reduce PGI_2-induced VASP phosphorylation. The phosphorylation of VASP was quantified by flow cytometry according to the manufacturer's instructions. The reduction of VASP phosphorylation induced by ADP was expressed as the % of PGI_2; the mean fluorescence intensity of PGI_2 plus ADP was devided by that of PGI_2.

Laboratory testing, ambulatory blood pressure monitoring, ankle-brachial index, and cardiorespiratory monitoring

Methods are described in detail in the supplementary materials. The intraassay and interassay coefficients of laboratory tests were all <10%. The data obtained from patients are shown in *Table 2*.

Statistical analysis

All statistical analyses were performed with SPSS version 11 software (SPSS, Inc., Chicago, IL, USA). The Mann–Whitney *U*-test was used to compare measurements of platelet activation between patients and healthy volunteers. The associations between the individual parameters were calculated using Spearman's correlation method. To identify independent factors, we used a step-wise multivariable linear regression analysis in which a *P*-value of 0.05 or less in a simple regression analysis was used as the criterion for entry into the model. We validated independent explanatory variables by Mann–Whitney *U*-test after categorization into two groups. All reported *P*-values are two-sided; a *P*-value of less than 0.05 was considered to be statistically significant.

Table 2 Physiological and biochemical characteristics of the study population

Biochemical markers	
White blood cells ($\times 1000\ mm^{-3}$)	7.1 ± 1.8
Haemoglobin (g/dL)	13.7 ± 1.8
Platelets ($\times 1000\ mm^{-3}$)	306.7 ± 84.0
Fasting glucose (mg/dL)	116.2 ± 46.7
Total cholesterol (mg/dL)	167.9 ± 35.6
Triglycerides (mg/dL)	130.9 ± 52.6
High-density lipoprotein cholesterol (mg/dL)	41.3 ± 11.8
Low-density lipoprotein cholesterol (mg/dL)	100.3 ± 29.5
Adrenalin (pg/mL)	31.1 ± 21.9
hsCRP (mg/L)	5.69 ± 7.60
Brain natriuretic peptide (pg/mL)	145.7 ± 174.7
PAI-1 (ng/mL)	56.6 ± 20.2
E-selectin (ng/mL)	20.4 ± 10.1
D-dimer (μg/mL)	1.8 ± 2.5
Soluble fibrin (μg/mL)	4.3 ± 7.5
Physiological markers	
24-h SBP (mmHg)	120.0 ± 14.5
24-h DBP (mmHg)	72.6 ± 9.1
24-h HR (b.p.m.)	68.2 ± 11.1
AHI ≥ 5/h, *n* (%)	75 (88)
AHI ≥ 15/h, *n* (%)	50 (59)
ABI	1.08 ± 0.123

Data for continuous variables are expressed as the mean ± SD.
hsCRP, high-sensitivity C-reactive protein; PAI-1, plasminogen activator inhibitor-1; SBP, systolic blood pressure; DBP, diastolic blood pressure; HR, heart rate; AHI, apnea–hypopnea index; ABI, ankle-brachial index.

Results

Patients

Of the 94 patients recruited, two were not included because of advanced gastric cancer or spastic angina, and three did not take dual antiplatelet drugs at the time blood was collected. An additional four patients were excluded from the analysis because of incomplete blood collection or failure of polysomnography or ABPM. Thus, 85 patients were finally included in the analysis (*Table 1*).

Dual antiplatelet therapy effectively inhibits its pharmacological targets

To precisely assess the effects of aspirin, we measured serum thromboxane B_2 (TxB_2) concentration, which reflects platelet-cyclooxygenase (COX)-dependent TxA_2 production. As has been described,[15,17] the serum TxB_2 concentration was uniformly abolished in all patients compared with control patients (*Figure 1A*). We also simultaneously evaluated VASP dephosphorylation after ADP stimulation, which reflects Gi-dependent cAMP reduction. As shown in *Figure 1B*, cAMP reduction by ADP was effectively

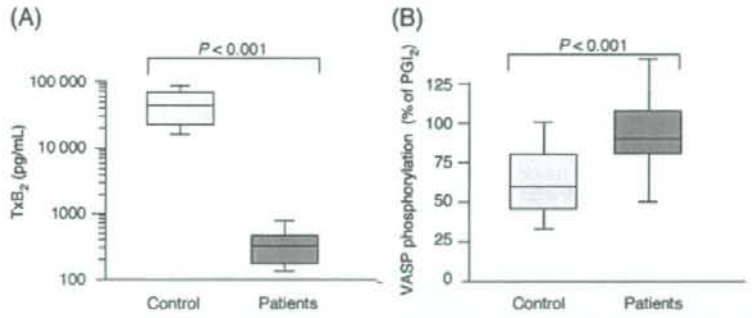

Figure 1 Serum thromboxane B_2 (TxB_2) concentration and vasodilator-stimulated phosphoprotein index in patients taking dual antiplatelet therapy. (*A*) The serum concentration of TxB_2 was measured by EIA. (*B*) The vasodilator-stimulated phosphoprotein phosphorylation was assessed by flow cytometry. ADP-induced vasodilator-stimulated phosphoprotein dephosphorylation was expressed as % of PGI_2. Data are expressed as box-and-whisker plots.

inhibited by dual antiplatelet therapy. These data suggested that dual antiplatelet therapy efficiently inhibits its pharmacological targets in patients undergoing PCI.

Inter-individual differences in platelet reactivity under dual antiplatelet therapy

Next, we examined the effects of dual antiplatelet therapy on platelet aggregation patterns using an aggregometry method that simultaneously measures both light transmission and light scattering. Although platelet aggregation assessed by light transmission was significantly decreased in the patients, the results of platelet aggregation tests induced by different agonists showed some inter-individual differences compared with serum TxB_2 and VASP phosphorylation (*Figure 2A*). We compared the changes of VASP phosphorylation and all platelet aggregations in the cilostazol group ($n = 10$) with those in the thienopyridine group ($n = 75$). We did not find any significant differences in platelet activation status, suggesting that drug differences could not explain the heterogeneity of platelet aggregation. Use of a laser-light scattering method to quantitatively evaluate the aggregate sizes and numbers revealed that the number of small aggregates increased after stimulation with all agonists, except for the lower concentration of ADP (*Figure 2B*). The inhibition of medium and large aggregates was clearer for low-dose agonist stimulation (data not shown), indicating that the platelet reactivity generating large platelet aggregates from small aggregates after agonist stimulation was highly concentration-dependent. Furthermore, the degrees of platelet aggregation induced by different agonists within a given subject significantly correlated with each other (*Table 3*). The number of small platelet aggregates spontaneously formed without agonist stimulation was significantly correlated with the collagen-induced platelet aggregation assessed by light transmission ($R = 0.398$, $P < 0.001$). We also found that small aggregate formation induced by a lower dose of agonist (1 μg/mL of collagen or 2 μM ADP) strongly correlated with light transmission induced by all higher concentrations of agonist ($R = 0.563–0.815$, $P < 0.001$). These data suggested that platelet aggregability under dual antiplatelet therapy may be determined by differences in the thresholds of each patient's platelets, rather than by differences in antiplatelet drug efficacies.

As activated platelets offer the scaffold of a coagulation cascade in arterial thrombus formation, we supposed that residual platelet activation under dual antiplatelet therapy may be involved in a systemic thrombin generation. To determine whether *in vitro* platelet aggregation is related to blood thrombogenicity, we compared the results of platelet aggregation tests with the plasma levels of SF (a marker for thrombin generation), D-dimer (a marker for fibrinolysis), PAI-1 (an inhibitor of fibrinolysis), and E-selectin (a marker for endothelial dysfunction). None of these variables was associated with the results of platelet aggregation (*Table 3*). Next, we attempted to determine factors influencing platelet aggregability by comparing the clinical backgrounds and other laboratory tests. Interestingly, we found that only the fasting glucose level was significantly correlated with the number of spontaneously formed small platelet aggregates and collagen-induced platelet aggregates ($R = 0.498$, $P < 0.001$ and $R = 0.243$, $P = 0.025$, respectively), regardless of the presence of diabetes mellitus (*Table 4*). Although many drugs including angiotensin-converting enzyme inhibitors, angiotensin II receptor blockers, and statin can influence platelet activation and blood coagulation, the use of these drugs did not affect the results of platelet aggregation tests, or the levels of PAI-1, D-dimer, SF, or E-selectin (data not shown).

Determinants of thrombin generation, fibrinolytic activity, and endothelial dysfunction

Finally, we examined the clinical characteristics that determine thrombin generation, fibrinolytic activity, and endothelial dysfunction. SF was significantly correlated with total cholesterol, BNP, ABI, and the number of coronary vessels affected *Table 4*. By multivariable regression analysis including these significant covariates,

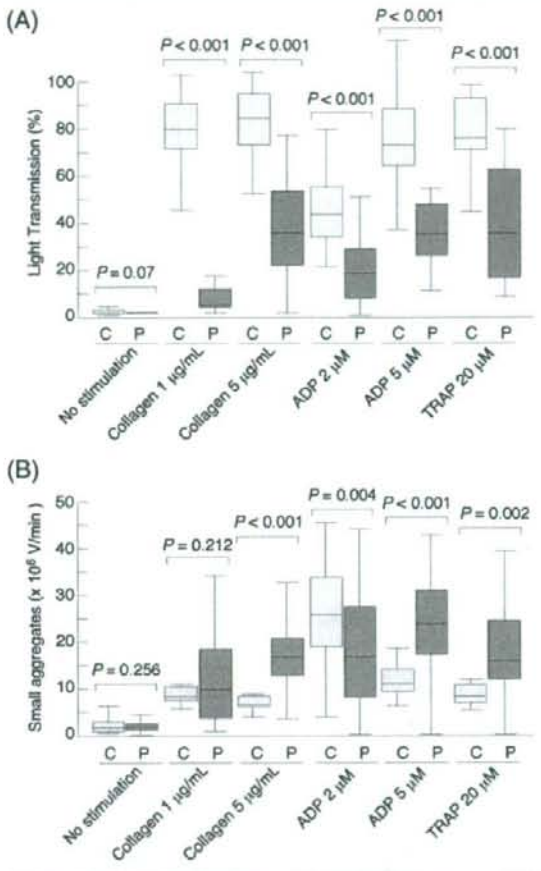

Figure 2 Platelet aggregation patterns in patients taking dual antiplatelet therapy. Platelets in platelet-rich plasma obtained from control subjects (*C*) or patients taking dual antiplatelet therapy (*P*) were stimulated with the indicated agonists for 5 min. (*A*) Changes in the maximum light transmission were monitored using conventional methods. (*B*) Light scattering intensities that represent small aggregate formation were measured simultaneously. Data are expressed as box-and-whisker plots.

total cholesterol, BNP, and ABI remained independently correlated with the SF level (*Table 5*). BNP was also an independent predictor of the D-dimer level in a multivariable regression analysis (*Table 5*). On the other hand, PAI-1 was significantly correlated with body mass index (BMI) and AHI *Table 4*. By multivariable analysis, only AHI remained independently correlated with the PAI-1 level (*Table 5*). E-selectin was significantly associated with age, BMI, diabetes mellitus, 24 h DBP, and AHI (*Table 4*). By multivariable regression analysis, BMI and diabetes mellitus remained independently correlated with the E-selectin level (*Table 5*). The significance of these explanatory variables was confirmed by Mann–Whitney *U*-test after categorization into two groups (see Supplementary material online, Figure S1). These results suggested that total thrombogenicity under antiplatelet therapy may be orchestrated by a variety of patient backgrounds that affect platelet reactivity, thrombin generation, fibrinolysis, and endothelial dysfunction.

Discussion

Activated platelets are critically involved in thrombotic complications after PCI and in acute coronary syndrome.[8–10] The issue of resistance to antiplatelet agents has been emphasized in the literature, leading to growing concern about the efficacy of antiplatelet therapy and about possible unfavorable clinical outcomes.[10–12] However, the term 'resistance' is frequently misleading when it refers to individuals who develop cardiovascular events despite antiplatelet therapy.[10–12] More accurately, we should properly

Table 3 Spearman's correlation coefficients among platelet aggregation (light transmission), PAI-1, D-dimer, SF, and E-selectin

	Collagen (1 µg/mL)	Collagen (5 µg/mL)	ADP (2 µg/ml)	ADP (5 µg/mL)	TRAP	PAI-1	D-dimer	Soluble fibrin
Collagen (1 µg/mL)	–	–	–	–	–	–	–	–
Collagen (5 µg/mL)	0.788 ($P < 0.001$)	–	–	–	–	–	–	–
ADP (2 µg/mL)	0.635 ($P < 0.001$)	0.853 ($P < 0.001$)	–	–	–	–	–	–
ADP (5 µg/mL)	0.608 ($P < 0.001$)	0.868 ($P < 0.001$)	0.931 ($P < 0.001$)	–	–	–	–	–
TRAP	0.417 ($P < 0.001$)	0.716 ($P < 0.001$)	0.646 ($P < 0.001$)	0.688 ($P < 0.001$)	–	–	–	–
PAI-1	−0.142 ($P = 0.194$)	−0.121 ($P = 0.271$)	−0.163 ($P = 0.137$)	−0.17 7 ($P = 0.105$)	−0.016 ($P = 0.884$)	–	–	–
D-dimer	0.050 ($P = 0.648$)	−0.007 ($P = 0.947$)	−0.007 ($P = 0.948$)	−0.047 ($P = 0.669$)	−0.177 ($P = 0.104$)	−0.169 ($P = 0.122$)	–	–
Soluble fibrin	0.100 ($P = 0.364$)	−0.046 ($P = 0.675$)	−0.022 ($P = 0.840$)	−0.021 ($P = 0.852$)	−0.170 ($P = 0.121$)	−0.061 ($P = 0.580$)	0.190 ($P = 0.082$)	–
E-selectin	−0.087 ($P = 0.427$)	−0.062 ($P = 0.572$)	−0.073 ($P = 0.506$)	−0.083 ($P = 0.049$)	0.031 ($P = 0.781$)	0.232 ($P = 0.032$)	0.042 ($P = 0.701$)	−0.105 ($P = 0.340$)

TRAP, thrombin receptor-activating peptide; PAI-1, plasminogen activator inhibitor-1.

distinguish patients who develop cardiovascular events despite antiplatelet therapy as 'treatment failure'.[30] From the viewpoint of Virchow's triad, arterial thrombosis may occur through complex interactions of a variety of components, including platelet activation, coagulation/fibrinolytic activity, endothelial dysfunction, and blood flow.[31,32]

On the basis of the results of our study, true antiplatelet drug resistance as defined by a specific test appears rare. This observation is consistent with recent studies, reporting that aspirin resistance other than non-compliance appears to be exceptional.[15–18,33] Although studies that used specific tests to measure the pharmacological effects of thienopyridines showed a wide variability in the responses to these drugs,[12] VASP dephosphorylation was significantly inhibited by dual antiplatelet therapy, and was not associated with ADP-induced platelet aggregation (data not shown). This discrepancy may be because of differences in the concentrations of ADP used; the commercially available VASP phosphorylation kit appears to use a high concentration of ADP (see Materials and Methods). As well, it is possible that pharmacokinetic differences related to race exist in the metabolism of thienopyridine antiplatelet drugs.

Although antiplatelet resistance has been defined by *in vitro* platelet function, there appears a widespread misunderstanding that *in vitro* platelet function directly represents inhibition of a drug target.[30] Here, we found that platelet aggregation elicited by different agonists were significantly correlated with each other and associated with small aggregate formation without or with lower agonist stimulation. These data suggest that the platelet aggregability under dual antiplatelet therapy may be determined by differences in the thresholds of each patient's platelets, rather than by differences in antiplatelet drug efficacies. Our finding is supported by recent reports that a 150 mg maintenance dose of clopidogrel is associated with enhanced antiplatelet effects compared with a 75 mg dose, although suboptimal responses were still present in 60% of patients.[34] Furthermore, Michelson *et al.*[35] reported that pre-existing variability in platelet responses to ADP accounts for clopidogrel resistance assessed by aggregometory.

We previously showed that an unknown factor, other than COX-1, determines inter-individual differences in platelet aggregation in aspirin-treated patients.[17] In this study, only fasting glucose level was significantly correlated with platelet aggregability, regardless of diabetes mellitus. Acute hyperglycemia during oral glucose tolerance tests was correlated with the number of small platelet aggregates.[28] Angiolillo *et al.*[34] reported that patients with hyperglycemia exhibit increased platelet reactivity, despite dual antiplatelet therapy, that continues to persist even after administration of a higher maintenance dose of clopidogrel. These findings indicate the importance of suppressing transient hyperglycemia by tight glucose control to prevent thrombotic complications after PCI. Indeed, elevated plasma glucose, with or without a diabetic status, was reportedly an independent predictor of outcomes in acute coronary syndrome patients.[36,37]

Treatment failure under antiplatelet drug therapy may be influenced by many factors. The coagulation cascade and its regulation are important contributors to clinical events after PCI.[19–21] Activated platelets provide phosphatidylserine exposure on their